Chemoselective Caging of Carboxyl Groups for On-Demand Protein Activation with Small Molecules

Yana D. Petri, Clair S. Gutierrez, and Ronald T. Raines*

[*] Y. D. Petri, C. S. Gutierrez, Prof. R. T. Raines
Department of Chemistry
Massachusetts Institute of Technology
Cambridge, Massachusetts 02139-4307, USA
E-mail: rtraines@mit.edu
Homepage: http://raineslab.com

1. General Information

Reaction Setup

Unless noted otherwise, reactions were performed under an atmosphere of N_2(g) using standard Schlenk-line techniques. Reactions carried out at low temperature were cooled in a Dewar vessel (water-ice bath at 0 °C), whereas reactions performed above room temperature were heated on the IKA RCT basic plate. All reaction mixtures were stirred magnetically and monitored by liquid chromatography–mass spectrometry (LC–MS) and by analytical thin-layer chromatography (TLC). Purification was done with flash column chromatography on silica gel. All diazoamide compounds were purified by a hand column to avoid any exposure to UV light from UV detectors. Organic solutions were concentrated *in vacuo* using a Buchi rotary evaporator (model R-210).

Solvent Removal

The phrase "concentrated under reduced pressure" refers to the removal of solvents and other volatile materials with a rotary evaporator at water-aspirator pressure of <20 Torr and a water bath at <25 °C. Residual solvents were removed from compounds by vacuum (<0.1 Torr) achieved by using a mechanical belt-drive oil pump.

Conditions

All procedures were performed at ambient temperature (~22 °C) and pressure (1.0 atm) unless indicated otherwise.

Chemical Reagents and Instrumentation

Reagents and solvents were from Sigma–Aldrich (Milwaukee, WI) and were used without further purification unless indicated otherwise. 1-Azido-4-iodobenzene was product #EN300-66112 from Enamine (Kyiv, Ukraine). Tri(2-furyl)phosphine was from TCI America (Portland, OR). *trans*-Cyclooctenol (**TCO-OH**) was from BroadPharm (San Diego, CA). Reagent-grade solvents—dichloromethane (DCM), tetrahydrofuran (THF), and triethylamine (Et_3N)—were dried over a column of alumina and removed from a dry still under an inert atmosphere. Anhydrous ethyl acetate (EtOAc) was from ACROS Organics (Geel, Belgium). Anhydrous dimethyl sulfoxide (DMSO) was from Sigma–Aldrich. $CDCl_3$ was from Cambridge Isotope Laboratories (Tewksbury, MA). Acetonitrile (MeCN) Optima LC/MS Grade was from Fisher Chemical (Waltham, MA). Flash column chromatography was performed with Silicycle 40−63 Å silica (230−400 mesh), and TLC was performed with EMD 250-μm silica gel 60 F254 plates. Potassium ferricyanide was from Sigma–Aldrich. 2-(*N*-Morpholino)ethanesulfonic acid (MES) was from Sigma–Aldrich.

Biological Reagents and Instrumentation

Lysozyme (Lyz) from chicken egg white (SKU: L4919-500MG; BioUltra, lyophilized powder, ≥98% by SDS–PAGE, ≥40,000 units mg^{-1} protein) was from Sigma–Aldrich. Concentrations of all proteins except Cyt *c* were determined using a bicinchonic acid (BCA) assay kit from Thermo

Fisher Scientific with an infinite M1000 plate reader from Tecan (Männedorf, Switzerland). The plate reader was also used for luminescence-based assays. The concentration of Cyt *c* was determined by absorbance at 410 nm for Cyt c heme *c* (extinction coefficient, ε_{max} = 106 $mM^{-1}\ cm^{-1}$)[1] with a DS-11 UV–vis spectrophotometer from DeNovix (Wilmington, DE). Amicon Ultra 0.5-mL centrifugal filters (10K) and (100K) were from Sigma–Aldrich. EnzCheck Lysozyme Assay Kit (product #E22013) was from Thermo Fisher Scientific. Kinetic fluorescence measurements for the EnzCheck assay were made with an infinite M1000 plate reader from Tecan. Endpoint fluorescence measurements for the EnzCheck assay were made with SpectraMax M5 plate reader from Molecular Devices (San Jose, CA). 96-well black, sterile microplates (product #6005660) from PerkinElmer (Waltham, MA) were used for fluorescent assays. Pepsin was product #V1959 from Promega (Madison, WI). DPBS with calcium and magnesium was product #14040141 from Gibco (Waltham, MA). Titer Plate Shaker was from Labline Instruments (Melrose Park, IL). Pig liver esterase (PLE) lyophilized powder with a specific activity of ≥50 units mg^{-1} solid (CAS Number: 9016-18-6, Product Number: 46058, 95.7 U/mg, Batch Number: BCCD7346) was from Sigma–Aldrich. Penicillin–streptomycin solution containing penicillin (10,000 units mL^{-1}) and streptomycin (10,000 μg mL^{-1}) was product #15140122 from Thermo Fisher Scientific (Waltham, MA). DMEM, powder, high glucose for M21 cells was product #12100046 from Thermo Fisher Scientific. Fetal Bovine Serum (FBS), Premium, US Sourced was product #45001-108 from Corning (Corning, NY). White, 384-well, flat-bottom plate was from Corning. Trypsin–EDTA (0.05%) with phenol red was from Thermo Fisher Scientific. Total protein concentration of M21 cell lysate was determined using a DS-11 UV–vis spectrophotometer from DeNovix (Wilmington, DE). The program Prism was from GraphPad (La Jolla, CA). Cytochrome *c* (Cyt *c*) from equine heart (C7752-50MG; ≥95% based on Mol. Wt. 12,384 basis) was from Sigma–Aldrich. Glu-C, sequencing grade was product #V1651 from Promega. Cytosolic extracts were obtained with a preparative Optima XE-90 ultracentrifuge from Beckman Coulter (Brea, CA). Complete Protease Inhibitor Cocktail Tablets were from Sigma–Aldrich. Spectra Multicolor Broad Range Protein Ladder was from Thermo Fisher Scientific. SDS–PAGE analyses were performed with Any kD™ Mini-PROTEAN® TGX™ Precast Gels in a Mini-PROTEAN Tetra cell from Bio-Rad Laboratories (Hercules, CA). Gels were imaged with an Amersham Imager 600 from GE Healthcare Life Sciences (Marlborough, MA). Cleaved caspase-3 (Asp175) rabbit antibody #9661, β-actin (D6A8) rabbit antibody #8457, and anti-rabbit IgG, HRP-linked antibody #7074, were from Cell Signaling (Danvers, MA). West Pico PLUS Chemiluminescent Substrate was from Thermo Fisher Scientific. HIV Protease FRET Substrate I (1 mg) was product #AS-22992 from AnaSpec (Fremont, CA). Caspase-Glo® 3/7 Assay System was product #G8090 from Promega. Caspase-Glo® 3/7 assays were performed using a Spark plate reader from Tecan. Isopropyl β-D-1-thiogalactopyranoside (IPTG; product #I2481C50) and ampicillin (product #A-301-25) were obtained from GoldBio (St Louis, MO). HIVPR purification was performed using an ÄKTA pure chromatography system with UNICORN software from Cytiva Life Sciences (Marlborough, MA). The columns used for HIVPR purification were a HiLoad 26/600 Superdex 75 pg column (product #28989334) and a HiTrap Q HP 1-ml column (product #29051325) from

Cytiva Life Sciences. The Amicon Stirred Cell 400mL (product #UFSC40001) and the 10kDa molecular weight cutoff ultrafiltration discs (product #PLGC07610) were from Sigma–Aldrich. Enzymatic assays with HIVPR were performed on a Spark plate reader from Tecan using black, half area 96 well plates (product #3993) from Corning (Sommerville, MA).

Nuclear Magnetic Resonance (NMR) Spectroscopy

^{1}H and ^{13}C NMR spectra were acquired with Bruker Avance Neo 400 MHz or 500 MHz spectrometers at the MIT Department of Chemistry Instrumentation Facility. Proton chemical shifts are reported in parts per million (ppm, δ scale) and are relative to residual protons in the deuterated solvent ($CDCl_3$: δ 7.26). Carbon chemical shifts are reported in parts per million (ppm, δ scale) and are relative to the carbon resonance of the solvent ($CDCl_3$: δ 77.2). Multiplicities are abbreviated as: s (singlet), br (broad), d (doublet), t (triplet), q (quartet), sept (septet), and m (multiplet). ^{13}C signal corresponding to diazo carbon (C=N=N) is missing in some spectra, possibly due to a T1 relaxation effect.[2]

Intact Mass Spectrometry (MS)

High-resolution mass spectrometry (HRMS) of small molecules was performed with an Agilent electrospray ionization (ESI) 6545 quadrupole time-of-flight (Q-TOF) mass spectrometer coupled to an Infinity 1260 LC system from Agilent Technologies (Santa Clara, CA). Intact masses of proteins and protein conjugates were accessed using an Agilent 6530C Accurate-Mass Q-TOF (Q-TOF 6530C) equipped with a PLRP-S column (1000 Å, 5-µm, 50 mm × 2.1 mm) from Agilent Technologies. Pepsin digests were analyzed on the Q-TOF 6530C equipped with a Poroshell 120 EC-C18 column (120 Å, 2.7-µm, 150 mm × 3.0 mm) from Agilent Technologies.

Absorbance Analysis

The Q-TOF 6530C was equipped with an 1290 Infinity II diode array detector (DAD) FS (G7117A) from Agilent Technologies. The DAD was used for absorbance analysis of Cyt *c* digests at 410 nm.

Sample Preparation for Intact MS with Q-TOF 6530C

Before analysis on the Q-TOF 6530C, all samples were diluted to 2 µM by total Lyz concentration (unless indicated otherwise) with Milli-Q water (0.1% v/v formic acid) and passed through a Spin-X Centrifugal Tube Filter (0.22-µm, cellulose acetate membrane) from R&D Systems (Minneapolis, MN).

Tandem Mass Spectrometry (MS/MS)

MS/MS analysis of the digested protein samples was performed on a NanoAcquity HPLC from Waters (Milford, MA) equipped with a self-packed Aeris C18 analytical column (20 cm × 0.075 mm) from Phenomenex (Torrance, CA). The eluent from the column was analyzed with an Orbitrap Elite mass spectrometer (nanospray configuration) from Thermo Fisher Scientific (Waltham, MA) operated in a data-dependent manner for 90 min.

Safety

Caution Although we have not encountered problems, diazo compounds are potentially explosive upon exposure to heat, light, pressure, and shock. They should be stored at ≤0 °C in the dark. *N*-Succinimidyl 2-diazoacetate (**S1**) is an exception, as it has been reported to be bench-stable and can be isolated in gram amounts as a crystalline solid.[3] α-Aryl-α-diazoesters structurally similar to **S1** have been shown to have T_{onset}, which reports on thermostability, ranging from 80 °C (*p*-OMe) to 130 °C (*p*-NO_2), depending on the aryl substituents.[4] Note that 1-azido-4-iodobenzene ($N_{carbon}/N_{nitrogen}$ ratio = 2) and diazo compounds **1** ($N_{carbon}/N_{nitrogen}$ ratio = 2) and **2** ($N_{carbon}/N_{nitrogen}$ ratio = 2) incorporate an aryl azide functionality, which is associated with additional explosive hazards (organic azides can also be heat, light, pressure, and shock-sensitive). Azides with a $N_{carbon}/N_{nitrogen}$ ratio between 1 and 3 can be isolated, "but they should be stored below room temperature at no more than 1 M concentration and at a maximum of 5 g of material."[5] Our synthetic routes (pages S7–S8) did not require any heat and were done on a small scale (<100 mg). Still, a blast shield should be placed around reaction vessels containing large amounts of potentially dangerous material. Furthermore, although we have concentrated solutions containing diazo compounds **1** and **2** under reduced pressure on a small scale, we recommend concentrating solutions containing large amounts of potentially dangerous material via an N_2(g) or Ar(g) stream.

Protein Structure Images

Images of protein structures were produced with the PyMOL software. The structure of hen egg Lyz was based on PDB entry 1hew.[6] The structure of Cyt *c* from horse heart was based on PDB entry 1hrc.[7] The structure of HIVPR was based on PDB entry 1f7a.[8]

Statistical Analysis

Unless indicated otherwise, statistical evaluation was performed by an unpaired Student's *t*-test with a one-sided *p* value.

2. Chemical Synthesis

2.1. Synthesis of *N*-Succinimidyl 2-Diazoacetate (S1)

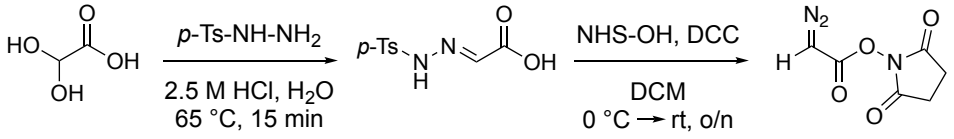

S1

***N*-Succinimidyl 2-diazoacetate (S1).** Compound **S1** was synthesized by following a reported synthetic route (without any modifications),[2] which was adapted from Wulff and coworkers[9] and Badet and coworkers.[3] **^{1}H NMR** (400 MHz, $CDCl_3$, δ): 5.11 (s, 1H), 2.85 (s, 4H). Note: The ^{1}H NMR spectrum of **S1** matched with that reported in the literature.[2]

2.2. Synthesis of Diazo Compound 1

The two-step synthesis of diazo compound **1** was adapted from previously reported conditions.[2]

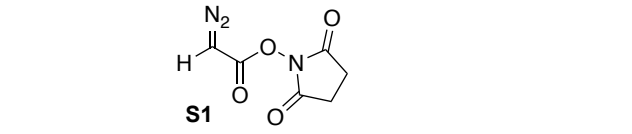

S1

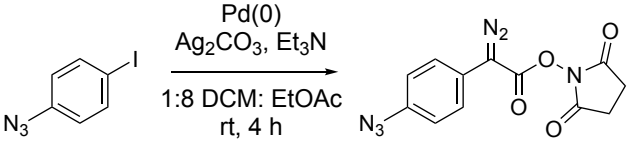

S2, 63%

2,5-Dioxopyrrolidin-1-yl 2-(4-azidophenyl)-2-diazoacetate (S2). S1 (15 mg, 0.082 mmol, 1.0 equiv), tri(furan-2-yl)phosphine (3.8 mg, 0.016 mmol, 20 mol %), and Ag_2CO_3 (11 mg, 0.041 mmol, 0.50 equiv) were added to a 20-mL vial charged with a magnetic stir bar. Subsequently, a solution of 1-azido-4-iodobenzene (20 mg, 0.082 mmol, 1.0 equiv) in 1:8 DCM/EtOAc (200 µL: 800 µL) was added to the reaction vial. A solution of Et_3N (17 µL, 0.12 mmol, 1.5 equiv) in EtOAc (400 µL) was then added, followed by rapid addition of a solution of $Pd(OAc)_2$ (2 mg, 0.0082 mmol, 10 mol %) in EtOAc (400 µL). The reaction mixture was stirred at room temperature for 4 h under N_2(g). The progress of the reaction was monitored by TLC. The reaction mixture was filtered through a Celite pad using a fitted syringe and washed with EtOAc. The filtrate was concentrated under reduced pressure and purified by silica gel chromatography (25% v/v EtOAc in hexanes) by hand to yield the title compound **S2** (15 mg, 0.052 mmol, 63% yield) as a yellow solid. Note that the reaction does not scale up well (the yield decreases), thus we advise setting up multiple small-scale reactions if larger amounts of **S2** are desired. **^{1}H NMR** (500 MHz, $CDCl_3$, δ): 7.41 (d, J = 8.7 Hz, 2H), 7.07 (d, J = 8.7 Hz, 2H), 2.88 (s, 4H). **^{13}C NMR** (126 MHz, $CDCl_3$, δ): 169.4, 160.4, 139.1, 130.2, 126.1, 120.1, 119.7, 25.7. **HRMS (ESI–TOF)**: Calc'd for $C_{12}H_9N_4O_4$ $[M–N_2 + H]^+$, 273.0618; found, 273.0590.

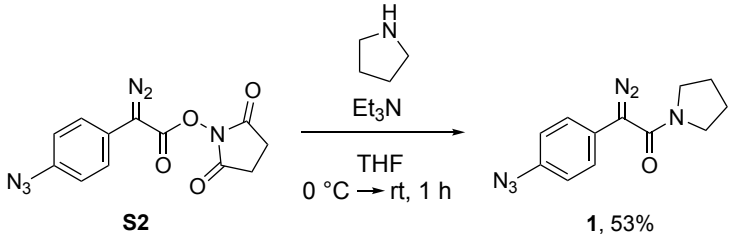

2-(4-Azidophenyl)-2-diazo-1-(pyrrolidin-1-yl)ethan-1-one (1). S2 (15 mg, 0.052 mmol, 1.0 equiv) was added to a 4-mL vial charged with a magnetic stir bar and dissolved in 0.5 mL of THF. A solution of Et_3N (14 µL, 0.10 mmol, 2.0 equiv) in THF (120 µL) was added to the reaction and cooled to 0 °C in an ice bath. A solution of pyrrolidine (7 mg, 0.10 mmol, 2.0 equiv) and Et_3N (14 µL, 0.10 mmol, 2.0 equiv) in THF (210 µL) was then added dropwise to the vial with **S2**. The reaction mixture was stirred at 0 °C for 20 min under ambient atmosphere and then allowed to warm to room temperature for another 40 min. The progress of the reaction was monitored by TLC, and product formation was indicated by the color of solution changing from yellow to darker orange. The reaction mixture was then filtered through a glass pipette fitted with a cotton plug, concentrated under reduced pressure, and purified by silica gel chromatography (23% v/v EtOAc in hexanes) by hand to afford diazo compound **1** (7.1 mg, 0.028 mmol, 53% yield) as an orange solid. **^{1}H NMR** (400 MHz, $CDCl_3$, δ): 7.32 (d, J = 8.7 Hz, 2H), 7.03 (d, J = 8.7 Hz, 2H), 3.45–3.42 (m, 4H), 1.93–1.89 (m, 4H). **^{13}C NMR** (101 MHz, $CDCl_3$, δ): 163.6, 137.7, 126.6, 123.8, 119.8, 48.0, 25.5. **HRMS (ESI–TOF)**: Calc'd for $C_{12}H_{13}N_4O$ $[M–N_2 + H]^+$, 229.10839; found, 229.1086. Note that the ^{13}C signal corresponding to diazo carbon (C=N=N) is missing in this spectrum, possibly due to a T1 relaxation effect.[2]

3. Lysozyme (Lyz) Caging with 1

3.1. Mechanism of Carboxyl Group Esterification by Diazo Compounds

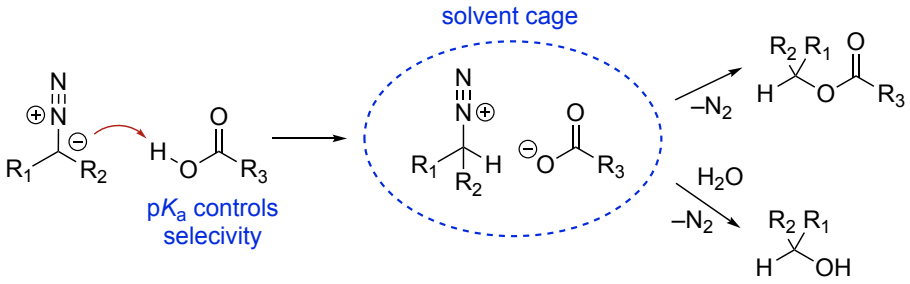

Figure S1. Putative mechanism of carboxyl group esterification by diazo compounds.[10] The first step is protonation of the diazo compound by acid, which leads to the formation of a diazonium·carboxylate ion pair, held within a solvent cage by a Coulombic force. The second step involves either a productive nucleophilic attack by the carboxylate to form an ester bond or non-productive hydrolysis.

3.2. Measured Literature pK_a Values of Carboxyl Groups in Lyz

Table S1. Measured literature pK_a values[11] of ten carboxyl groups in Lyz from chicken egg white sorted in descending order. An active-site residue, Glu35 (highlighted in blue), has a pK_a value that is more than two units greater than that of other carboxyl groups in Lyz. Note that Asp52, another active-site residue, has the third highest pK_a.

Lyz Carboxyl Group	Measured pK_a
E35	**6.2**
D101	4.09
D52	3.68
D119	3.20
E7	2.85
C-terminus	2.75
D18	2.66
D87	2.07
D48	1.6
D66	0.9

3.3. pH and Equivalents Screen for Optimal Lyz Caging Conditions

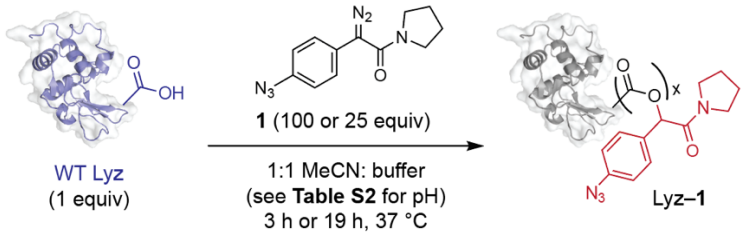

To a solution of WT Lyz (500 µM, 1.0 equiv) in aqueous buffers of varying pH (see Figure S2 for details) was added a solution of **1** (50 mM, 100 or 25 equiv per WT protein, which is 10 or 2.5 equiv per carboxyl group, respectively) in MeCN (50% v/v). The reactions were incubated at 37 °C with mild shaking (speed 1.5 on Titer Plate Shaker). The number of ester labels on the resultant crude protein conjugates (Lyz–**1**) was accessed via Q-TOF MS (Figures S2A and S2B) after 3 h. Reactions carried out at pH 6.5 and 7.0 were incubated for another 16 h and buffer-exchanged into DPBS with calcium and magnesium (×3) using Amicon Ultra 0.5-mL centrifugal filters (10K). The number of ester labels on the resultant buffer-exchanged Lyz–**1** conjugates was assessed by using Q-TOF MS (Figure S2C). See Table S2 for the percentage of Glu35 (target active-site residue) and Asp101 (off-target residue with closest pK_a to Glu35) protonated at the relevant pHs at equilibrium as well as the ratio of their protonated states.

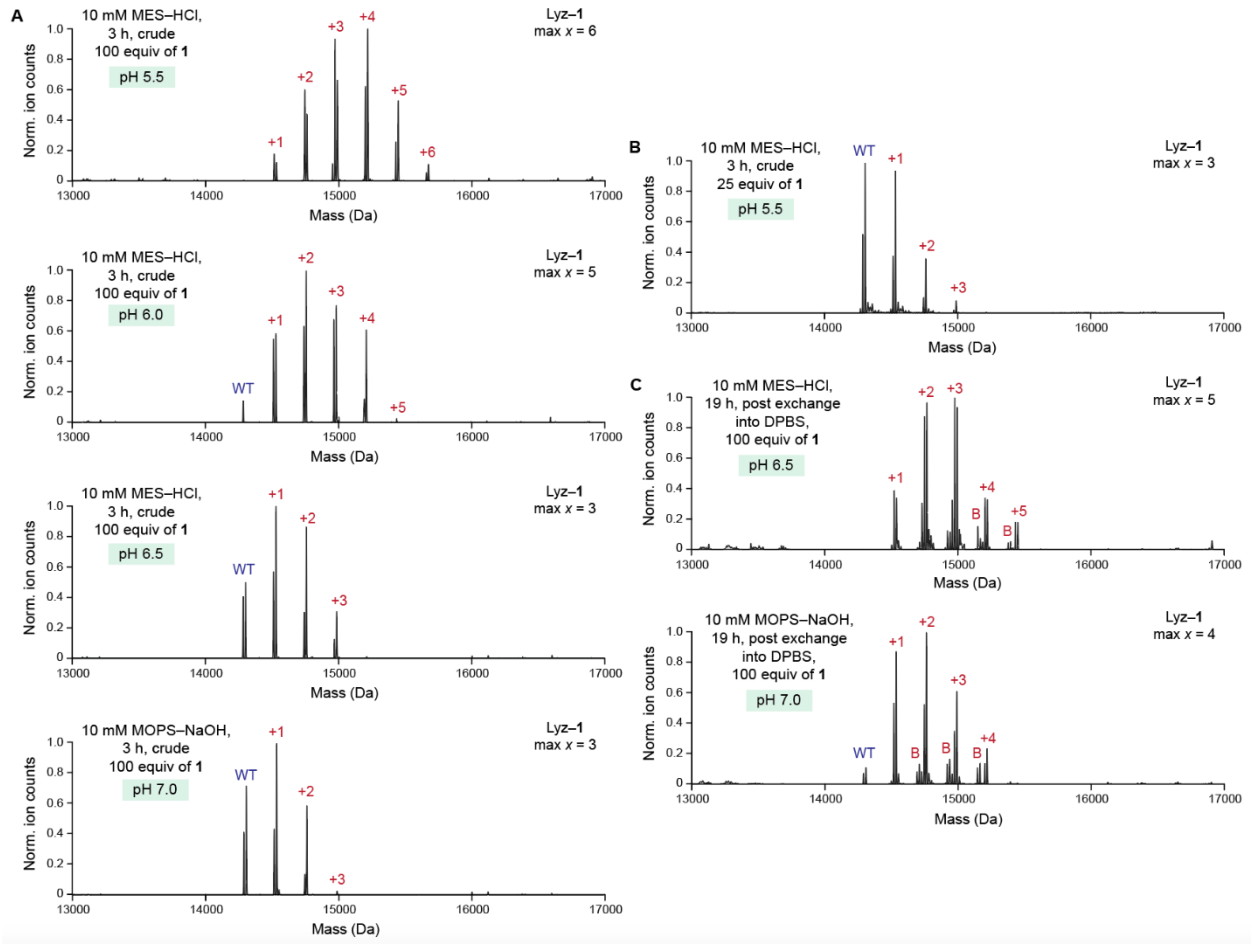

		WT Lyz	+1	+2	+3	+4	+5	+6
Lyz–**1**	Exp'd MW	14305	14533	14761	14989	15217	15445	15673
(+228 Da/label)	Obs'd MW	14305	14533	14761	14990	15218	15447	15674

***Figure S2*. Top.** A. Deconvoluted Q-TOF mass spectra of crude solutions of Lyz–**1** synthesized in buffers of varying pH for 3 h using 100 equiv of **1**. B. Q-TOF mass spectrum of the crude solution of Lyz–**1** synthesized at pH 5.5 for 3 h using 25 equiv of **1**. C. Deconvoluted Q-TOF mass spectra of Lyz–**1** synthesized in buffers of varying pH for 19 h using 100 equiv of **1** and later exchanged into DPBS. "Max *x*" refers to the maximum number of carboxyl groups esterified in Lyz–**1**. The ion intensity was normalized (norm.) so that the ordinate of the highest point is equal to 1. **Bottom.** List of expected (exp'd) and observed (obs'd) masses. "B" refers to an unknown byproduct that reacts with Lyz upon prolonged incubation of the protein with diazo compound **1**. "WT" refers to the native protein.

Table S2. Buffers chosen for the esterification of Lyz with diazo compound **1**, their pH, and the percentage and ratio of protonated Glu35 and Asp101 calculated to form at equilibrium using the Henderson–Hasselbalch equation.

Buffer	pH	% Protonated Glu35	% Protonated Asp101	% Protonated Glu35/Asp101
10 mM MES–HCl	5.5	83	3.7	22
10 mM MES–HCl	6.0	61	1.2	51
10 mM MES–HCl	6.5	33	0.39	85
10 mM MOPS–NaOH	7.0	14	0.12	117

3.4. Synthesis of the Optimally Caged Lyz (Lyz–1)

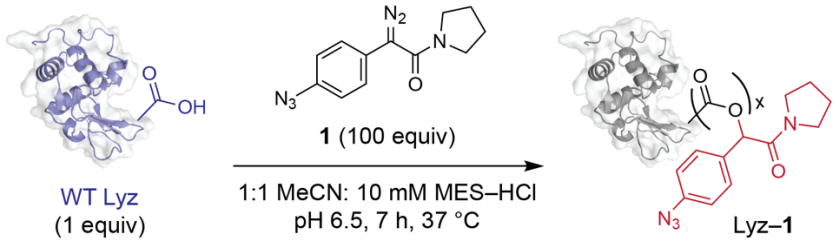

To a solution of WT Lyz (500 µM, 1.0 equiv) in 10 mM MES–HCl buffer, pH 6.5, was added a solution of diazo compound **1** (50 mM, 100 equiv per protein or 10 equiv per carboxyl group) in MeCN (50% v/v). The reaction mixture was incubated for 7 h at 37 °C with mild shaking (speed 1.5 on Titer Plate Shaker). Subsequently, the reaction solution was buffer-exchanged into DPBS with calcium and magnesium (3×) using Amicon Ultra 0.5-mL centrifugal filters (10K). The number of ester labels on the resultant buffer-exchanged Lyz–**1** conjugate was assessed by using Q-TOF MS (Figure S3).

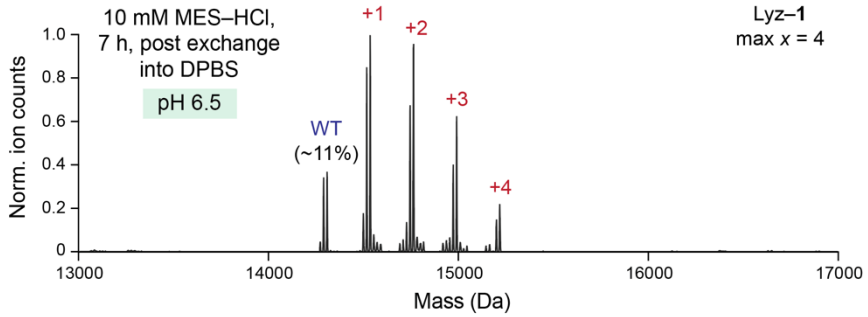

Figure S3. Q-TOF mass spectrum of optimally caged Lyz–**1**, which was buffer-exchanged into DPBS after 7 h. "Max *x*" refers to the maximum number of carboxyl groups esterified in Lyz–**1**. The ion intensity was normalized (norm.) so that the ordinate of the highest point is equal to 1. Note that, in addition to peaks that correspond to the expected ester labels of diazo compound **1**, we also observed adjacent peaks that correspond to a loss of 16, 18, or 19 Da, which is likely a mass spectrometry artifact. A truncated version of these data is depicted in Figure 2B.

4. Identification of Esterified Carboxyl Groups in Lyz–1

4.1. Determination of Relative k_{cat} and K_M Values of WT Lyz and Lyz–1

The EnzCheck Lysozyme Assay Kit was used to determine the k_{cat} and K_M of WT Lyz and optimally caged Lyz–**1** (synthesized at pH 6.5 as described in Section 3.4). This assay measures the activity of Lyz on *Micrococcus lysodeikticus* cell walls, which are labeled with fluorescein to such a degree that fluorescence is quenched. Lyz can cleave the β-1,4 glycosidic bonds in the cell walls, relieving the quenching and yielding an increase in fluorescence that is proportional to enzymatic activity. Bacterial cell wall concentrations were varied by twofold dilutions ranging from 192 μg mL^{-1} to 0.75 μg mL^{-1}. A final concentration of 1 μM was used for WT Lyz and Lyz–**1**. Assays were performed in quadruplicates in black 384-well plates (20-μL final volume per well) on a Tecan M1000 plate reader using excitation and emission wavelengths of 485 nm and 530 nm, respectively. Briefly, 10 μL of 2× cell wall substrate was added to the relevant wells and a blank measurement was recorded after 5 min to establish baseline fluorescence (I_0). Then, 10 μL of a 2× solution of WT Lyz or Lyz–**1** was added to each well and read at 30-s intervals for 3 h. To ensure that the reactions went to completion, a 100-μM solution of WT Lyz was added to another set of wells for each tested cell wall concentration to establish the maximum product fluorescence, (I_{max}), which was averaged over four replicates. To convert raw fluorescence values to product concentration, a linear relationship between fluorescence and product concentration was assumed. Eq 1 was used to fit each time point:

$$[\mathrm{P}] = \frac{I - I_0}{I_{\mathrm{max}} - I_0}[\mathrm{S}_0] \tag{1}$$

Where I is the fluorescence of a given well at a given time point and $[S_0]$ is the initial concentration of substrate (μg mL^{-1}). To calculate the initial rate of each progress curve, a linear regression was applied to the first 30 datapoints (recorded within 5 min) and the fitted slope was used as the initial rate. Since the reactions proceeded slowly, this region was approximately linear. The resultant initial rates were then fitted by non-linear regression to the Michaelis–Menten equation[12] (Eq 2) using a Python script to obtain the k_{cat} and K_M.

$$v = \frac{\mathrm{d}[\mathrm{P}]}{\mathrm{d}t} = \frac{k_{\mathrm{cat}}[\mathrm{E}][\mathrm{S}_0]}{K_{\mathrm{M}} + [\mathrm{S}_0]} \tag{2}$$

Errors were reported as the 95% confidence interval and were calculated by converting the covariance of the optimally fitted parameters (from the curve fitting function used) and adjusting to a 95% confidence interval using Eq 3:

$$\mathrm{SE}_{95} = \sqrt{\mathrm{COV}} * Z_{95} \tag{3}$$

where

COV = Fit covariance
Z_{95} = Z value for a 95% confidence interval = 1.96

Code and datasets used are available at https://github.com/clair-gutierrez/MM_lysozyme_caging. The results are shown in Figure 2C.

4.2. Intact MS Analysis of Pepsin Digests of Lyz–1

General Note on the Stability of Ester Bonds in Esterified Proteins

Based on empirical observations and previous studies,[2] ester bonds produced between proteins and diazo compounds such as **1** are more suspectable to hydrolysis at (1) higher temperatures, and (2) higher pH (*e.g.,* such ester bonds are more labile at pH 8.0 rather than pH 5.8). Thus, to maximize the preservation of ester bonds, we avoided subjecting esterified conjugate to neutral or basic conditions and incubations at temperatures above 37 °C during denaturation and subsequent digestion. These precautions were behind our choice of pepsin as the digestion enzyme (since its optimal cleavage performance is at pH 1–3) and behind the use of 0.1% v/v formic acid in Milli-Q water (final pH of 2.8) as the denaturation reagent.

Denaturation and Pepsin Digestion

WT Lyz was labeled with **1** at pH 6.5 (for 7 h, as described on page S11) or pH 5.5 (for 4 h, as described on pages S9–S11) and buffer-exchanged into DPBS. To denature the protein and achieve a pH optimum of pepsin (pH 1–3), Lyz–**1** (20 μg, 14 μL of a 99 μM stock solution in DPBS) was diluted with 186 μL of Milli-Q water and 2 μL of Milli-Q water containing 10% v/v formic acid. A fresh stock solution of 0.01 mg^{-1} mL pepsin, which was product #V1959 from Promega, was prepared in Milli-Q water containing 0.1% v/v formic acid. This pepsin stock solution (1 μg, 100 μL) was then added to the solution of Lyz–**1** (202 μL) to achieve a pepsin:substrate (Lyz–**1**) w/w ratio of 1:20. The samples were incubated for 30 min or 1 h at 37 °C with mild shaking (speed 1.5 on Titer Plate Shaker). Pepsin activity was halted by freezing the samples in liquid N_2. The samples were stored at −80 °C and analyzed by Q-TOF MS immediately upon thawing.

Note on Disulfide Scrambling in Lyz

Although Lyz contains four disulfide bonds,[13] we did not purposefully reduce them prior to digestion. Since some aryl azides (and possibly ester labels of **1**) are suspectable to reduction by dithiothreitol[14] and tris(2-carboxyethyl)phosphine,[15] we avoided the use of these reagents. It has been previously shown that proteolysis of Lyz with pepsin under acidic conditions does not eliminate disulfide scrambling, which results in the formation of a detectable pool of free thiols.[16]

Intact Q-TOF MS Analysis

The digested samples were rapidly thawed and immediately analyzed on the Q-TOF 6530C equipped with a Poroshell 120 EC-C18 column as described on page S5. A gradient of 5–40% v/v MeCN (0.1% v/v formic acid) in Milli-Q water (0.1% v/v formic acid) over 15 min was used and the column was pre-heated to 60 °C. Masses of the pepsin digests were analyzed in the program BioConfirm B.09.00 from Agilent Technologies. Peptides were searched against the sequence of "reduced" WT Lyz. The Protein Digest workflow was followed with "nonspecific" defined as the cleavage enzyme, since pepsin has broad specificity with a preference for hydrophobic residues at P1 and P1′ positions.[17] Labels of **1** were defined as variable modifications (monoisotopic delta mass: +228.101111, gain of $C_{12}H_{13}N_4O$ and loss of H, specificity for E and D residues, up to 10 modifications per protein). Protein digest MS match tolerance was set to ≤3 ppm and the allowed charge states were +1 and +2. Peaks with peak heights of <1000 counts were excluded from the analysis. Only peptides esterified at a single carboxyl group were reported as esterified for higher confidence. Peak areas were calculated by integrating the peaks in the program Qualitative Analysis B.07.00 from Agilent Technologies. All esterified peptides detected within the aforementioned constraints were reported. The results are shown in Figures S4 and S5.

```
1         10        20        30        40        50        60
KVFGRCELAAAMKRHGLDNYRGYSLGNWVCAAKFESNFNTQATNRNTDGSTDYGILQINS

          70        80        90        100       110       120
RWWCNDGRTPGSRNLCNIPCSALLSSDITASVNCAKKIVSDGNGMNAWVAWRNRCKGTDVQAWIRGCRL
```

Peptide	Esterified Residue	Peak Area	|Ppm|
F**E**SN	**E35**	2.7×10^5	0.37
KF**E**	**E35**	5.7×10^4	1
AKF**E**SNF	**E35**	5.6×10^4	2.4
GL**D**NYRGYSLGNWVC	D18	8.3×10^4	3
NTQATNRNT**D**GST**D**YGIL	D48 or D52	3.9×10^4	2.1
DYGILQI	D52	1.3×10^4	2.5
SS**D**ITA	D87	9.6×10^3	0.22
LSS**D**ITA	D87	9.7×10^3	2.8

***Figure S4*. Top.** Sequence coverage of Lyz–**1** (WT Lyz esterified with **1** at pH 6.5) identified by Q-TOF MS post a 1-h pepsin digest. Portions of the sequence that were not detected are highlighted in red. Esterified Glu35 is bolded in blue; other unambiguously esterified residues are bolded in green; a possibly esterified residue is bolded in orange. **Bottom.** Esterified residues are listed in the order from most abundant to least abundant in terms of peak area.

Analysis: Overall, peptides esterified at Glu35, which is the Lyz active-site residue with an elevated pK_a, are the most abundant in this dataset. Further, peptides esterified at Glu35 are at least 7-fold more abundant than peptides esterified at Asp52, the second active-site residue of Lyz.

1 10 20 30 40 50 60
KVFGRC**E**LAAAMKRHGL**D**NYRGYSLGNWVCAAKF**E**SNFNTQATNRNT**D**GST**D**YGILQINS

70 80 90 100 110 120
RWWCN**D**GRTPGSRNLCNIPCSALLSS**D**ITASVNCAKKIVS**D**GNGMNAWVAWRNRCKGTDVQAWIRGCRL

Peptide	Esterified Residue	Peak Area	|Ppm|
SALLSS**D**I	D87	4.0×10^5	1.3
S**D**ITASVNCAKKIVS**D**	D87 or D101	2.5×10^4	0.52
LSS**D**ITA	D87	1.0×10^4	1.8
SS**D**ITA	D87	1.0×10^4	0.86
MKRHGL**D**NYRGYSL	D18	2.5×10^5	2.2
KVFGRC**E**LAAAMKRHGL**D**NY	E7 or D18	5.1×10^3	2.2
F**E**SN	**E35**	1.9×10^5	0.42
KF**E**	**E35**	5.5×10^4	0.46
AKF**E**SNF	**E35**	3.0×10^4	2.1
VFGRC**E**L	E7	1.4×10^5	0.96
C**E**LAAAMK	E7	7.7×10^3	1.8
QINSRWWCN**D**GR	D66	5.7×10^4	2.9
NTQATNRNT**D**GST**D**YGIL	D48 or D52	4.9×10^4	1.8
ASVNCAKKIVS**D**GNGMN	D101	1.9×10^4	0.53
TNRNT**D**G	D48	1.7×10^4	2.5
WWCN**D**GRTPGSRNLC	D66	1.3×10^4	3

***Figure S5*. Top.** Sequence coverage of Lyz–**1** (WT Lyz esterified with **1** at pH 5.5) identified by Q-TOF MS post a 30-min pepsin digest. Portions of the sequence that were not detected are highlighted in red. Esterified Glu35 is bolded in blue; other unambiguously esterified residues are bolded in green; a possibly esterified residue is bolded in orange. **Bottom.** Esterified residues are listed in the order from most abundant to least abundant in terms of peak area.

Analysis: Together, the datasets in Figures S4 and S5 demonstrate that the abundance of peptides esterified at Glu35 is a function of pH. Further, the dataset in Figure S5 shows that, in general, more Glu and Asp residues can get labeled by diazo compound **1** at a lower pH, which indicated decreased specificity.

4.3. Tandem MS (MS/MS) Analysis of Pepsin Digests of Lyz–1

Denaturation and Pepsin Digestion

Pepsin digests of optimally caged Lyz–**1** (WT Lyz esterified with **1** at pH 6.5) for MS/MS analysis were prepared as described on page S13.

Orbitrap MS/MS Analysis

The digested samples were rapidly thawed and immediately subjected to MS/MS analysis as described on page S14. Briefly, the samples were injected onto a NanoAcquity HPLC from Waters equipped with a self-packed Aeris C18 analytical column. Peptides were eluted using standard reverse-phase gradients. The effluent from the column was analyzed using an Orbitrap Elite mass spectrometer (nanospray configuration) from Thermo Fisher Scientific operated in a data-dependent manner for 90 min. The resulting fragmentation spectra were correlated against a known database using PEAKS Studio 10 from Bioinformatic Solutions (Ontario, Canada) to provide consensus reports for the identified proteins. MS/MS peptide identifications were reported using the 1% False Discovery Rate (FDR) cutoff. Protein digest MS match tolerance was set to ≤3 ppm. Note that singly charged peptides do not fragment well[18] and thus there is often an insufficient number of MS/MS ions to get a match within the 1% FDR cutoff. The results are in Figure S6.

```
1         10        20        30        40        50        60
KVFGRCELAAAMKRHGLDNYRGYSLGNWVCAAKFESNFNTQATNRNTDGSTDYGILQINS

          70        80        90       100       110       120
RWWCNDGRTPGSRNLCNIPCSALLSSDITASVNCAKKIVSDGNGMNAWVAWRNRCKGTDVQAWIRGCRL
```

Peptide	Esterified Residue	Peak Area	|Ppm|
FNTQATNRNTDGST**D**YGILQ	D52	4.2×10^8	2.7
FNTQATNRNTDGST**D**YG	D52	3.7×10^6	1.6
QATNRNTDGST**D**YGILQ	D52	2.7×10^6	1.4
FNTQATNRNTDGST**D**Y	D52	2.6×10^6	0.8
ATNRNTDGST**D**YGILQ	D52	1.3×10^6	1.5
FNTQATNRNTDGST**D**YGILQIN	D52	8.4×10^5	2.4
FNTQATNRNT**D**GSTDYGILQ	D48	7.8×10^5	1.6

Figure S6. **Top.** Sequence coverage of Lyz–**1** (WT Lyz esterified with diazo compound **1** at pH 6.5) identified by Orbitrap MS/MS post a 1-h pepsin digest. Portions of the sequence that were not detected are highlighted in red. Unambiguously esterified residues are bolded in green. **Bottom.** Esterified residues are listed from most abundant to least abundant in terms of peak areas.

Analysis: This dataset was not usable because it produced a poor sequence coverage. It is also possible that the process of collision-induced dissociation (CID) used for fragmentation of amide bonds in this sample also resulted in undesirable fragmentation of some ester bonds.

5. Lyz–1 Decaging with Small Molecules

5.1. Lys–1 Decaging with 2-(Diphenylphosphino)benzoic Acid (2-DPBA)

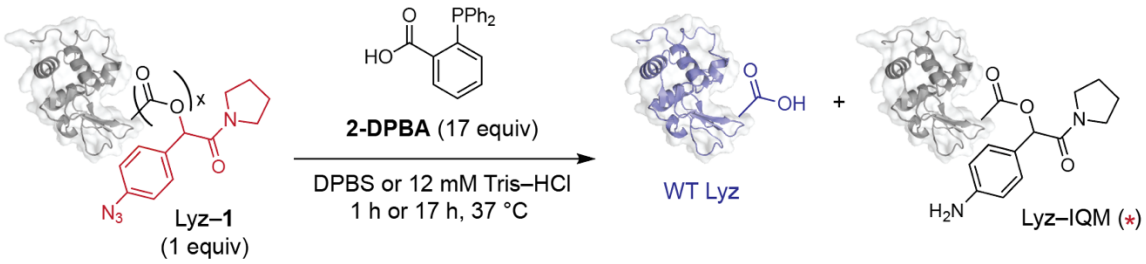

WT Lyz was labeled with **1** at pH 6.5 (for 7 h, as described on page S11) and buffer-exchanged into DPBS (Figure S7A). A fresh 5-mM stock solution of 2-DPBA in 1:1 MeCN/DPBS was then prepared. To initiate decaging, the 5-mM stock solution of 2-DPBA (17 equiv, 1.6 µL) was added to a solution of Lyz–**1** (1 equiv, 14.4 µL, 33 µM) in DPBS. The reaction mixture was incubated for 1 h at 37 °C with mild shaking (speed 1.5 on Titer Plate Shaker) and checked by Q-TOF MS (Figure S7B). Efficient release of WT Lyz was observed in addition to a byproduct that likely resulted from the incomplete elimination of the aniline intermediate from a carboxyl group (Lyz–IQM, where IQM stands for imino-quinone methide). To test the reversibility of this byproduct, the reaction mixture was incubated for another 16 h at 37 °C with mild shaking and checked by Q-TOF MS (Figure S7C). Only WT Lyz was observed in this experiment, which confirmed that Lyz–IQM is susceptible to cleavage. Note that we also performed the decaging reaction (same conditions as above) in 12 mM Tris–HCl (pH 7.4) instead of DPBS and observed a similar amount of Lyz–IQM as in Figure S7B (Figure S7D). This experiment provided evidence that the eliminated IQM does not alkylate Lys residues in Lyz.

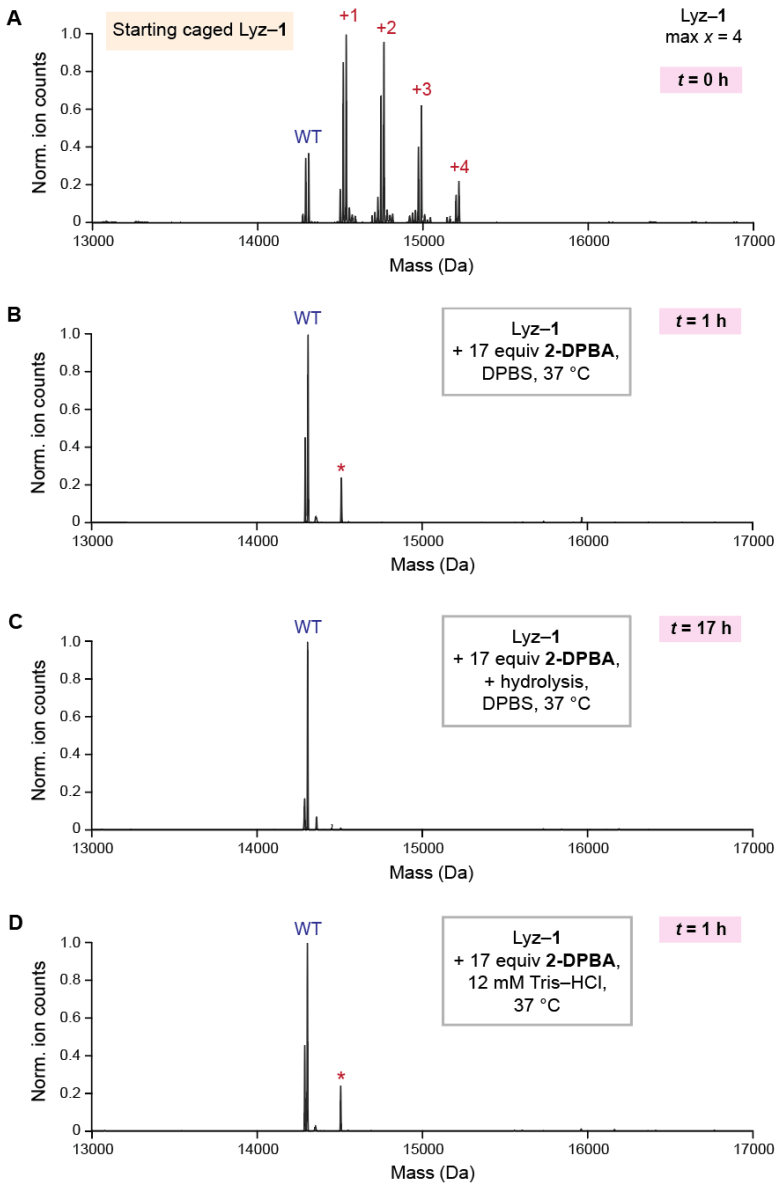

		WT Lyz	+1
Lyz–IQM	Exp'd MW	14305	14507
(+202 Da/label)	Obs'd MW	14305	14507

Figure S7. **Top.** Deconvoluted Q-TOF mass spectra of (A) the starting Lyz–**1** conjugate, (B) Lyz–**1** decaged with 2-DPBA and spontaneous hydrolysis for 1 h, (C) Lyz–**1** decaged with 2-DPBA and spontaneous hydrolysis for 17 h, and (D) Lyz–**1** decaged with 2-DPBA in the presence of excess amines in the Tris buffer and spontaneous hydrolysis for 1 h. "Max *x*" refers to the maximum number of carboxyl groups esterified in Lyz–**1**. The ion intensity was normalized (norm.) so that the ordinate of the highest point is equal to 1. The red asterisk refers to Lyz–IQM. **Bottom.** List of expected (exp'd) and observed (obs'd) masses. Truncated versions of Figures S7A–C are depicted in Figures 2B, 3B, and 3C, respectively.

5.2. Lys–1 Decaging with *trans*-Cyclooctenol (TCO-OH)

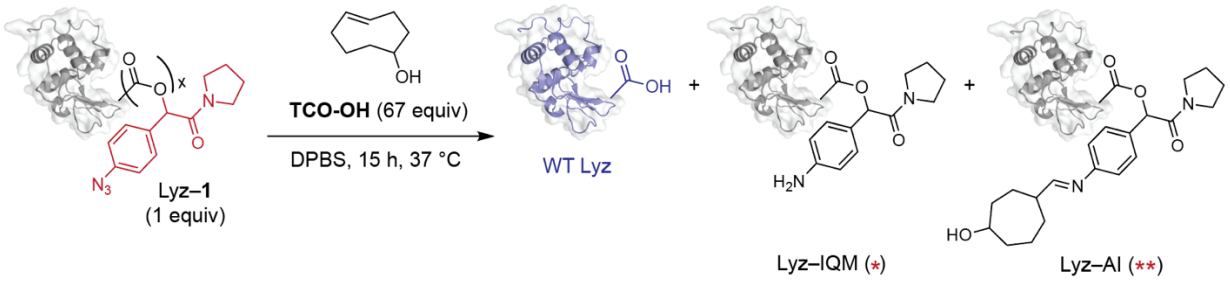

WT Lyz was labeled with **1** at pH 6.5 (for 7 h, as described on page S11) and buffer-exchanged into DPBS (Figure S8A). To control for background hydrolysis of the esters, Lyz–**1** was incubated in DPBS for 15 h at 37 °C with mild shaking (speed 1.5 on Titer Plate Shaker) and checked by Q-TOF MS (Figure 8B). Up to 3 esters labels (max $x = 3$) on Lyz–**1** were intact in this control sample. A fresh 5-mM stock solution of TCO-OH in 1:19 DMSO/DPBS was then prepared. To initiate decaging, the 5-mM stock of TCO-OH (67 equiv, 6.4 µL) was added to a solution of Lyz–**1** (1 equiv, 9.6 µL, 50 µM) in DPBS. The reaction mixture was incubated for 15 h at 37 °C with mild shaking and immediately checked by Q-TOF MS (Figure 8C). Efficient release of WT Lyz was observed in addition to the Lyz–IQM byproduct and a byproduct of incomplete hydrolysis of the aldimine intermediate that formed upon TCO-OH cycloaddition with Lyz–**1** (Lyz–AI).

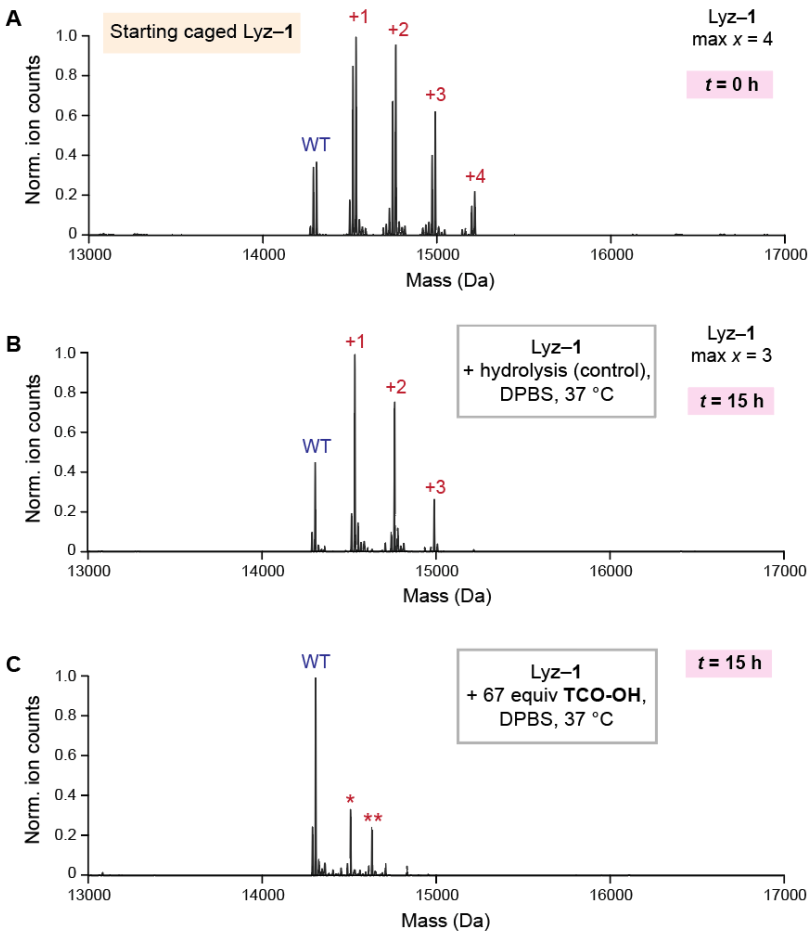

		WT Lyz	+1
Lyz–**IA**	Exp'd MW	14305	14632
(+327 Da/label)	Obs'd MW	14305	14631

***Figure S8*. Top.** Deconvoluted Q-TOF mass spectra of (A) the starting Lyz–**1** conjugate, (B) Lyz–**1** subjected to spontaneous hydrolysis for 15 h, and (C) Lyz–**1** decaged with TCO-OH and spontaneous hydrolysis for 15 h. "Max *x*" refers to the maximum number of carboxyl groups esterified in Lyz–**1**. "WT" refers to the native protein. The ion intensity was normalized (norm.) so that the ordinate of the highest point is equal to 1. The red asterisk refers to Lyz–IQM. Two red asterisks refer to Lyz–AI. **Bottom.** List of expected (exp'd) and observed (obs'd) masses. Truncated versions of Figures S8A and S8C are depicted in Figures 2B and 3D, respectively.

6. Activity of Lyz on *Micrococcus lysodeikticus* Cell Walls

WT Lyz was labeled with **1** at pH 6.5 (for 7 h, as described on page S11) and buffer-exchanged into DPBS. The Lyz–**1** conjugate was decaged with 2-DPBA alone (pages S17–S18), with 2-DPBA and hydrolysis (pages S17–S18), or with TCO-OH alone (pages S19–S20). The decaged samples were buffer-exchanged into DPBS (3×) using Amicon Ultra 0.5-mL centrifugal filters (10K). To compare the relative activities of WT Lyz, Lyz–1, and the decaged samples, the EnzCheck Lysozyme Assay Kit was used at the final concentration of 0.125 μM or 0.25 μM of Lyz per well. Briefly, experimental samples of Lyz were diluted to 0.25 μM or 0.5 μM with 1× reaction buffer from the kit and 50-μL aliquots of these solutions were added into wells of a black 96-well plate. 50-μL aliquots of the 1× reaction buffer alone were added to separate wells to control for background fluorescence. A 50 μg mL^{-1} suspension of the cell wall substrate was then prepared in the 1× reaction buffer and 50-μL aliquots of this stock were rapidly added to each well containing experimental or control samples. The assays were performed in technical triplicates. The reactions were incubated for 37 °C for 30 min. Endpoint fluorescence intensity of each well was then measured on a SpectraMax M5 plate reader using fluorescence absorption and emission wavelengths of 494 nm and 518 nm, respectively. The average fluorescence intensity of the controls was subtracted from the average fluorescence intensity of the experimental samples and the resultant values were normalized so that the activity of WT Lyz was equal to 100%. The results of the assays plotted in the program Prism are shown in Figure S9.

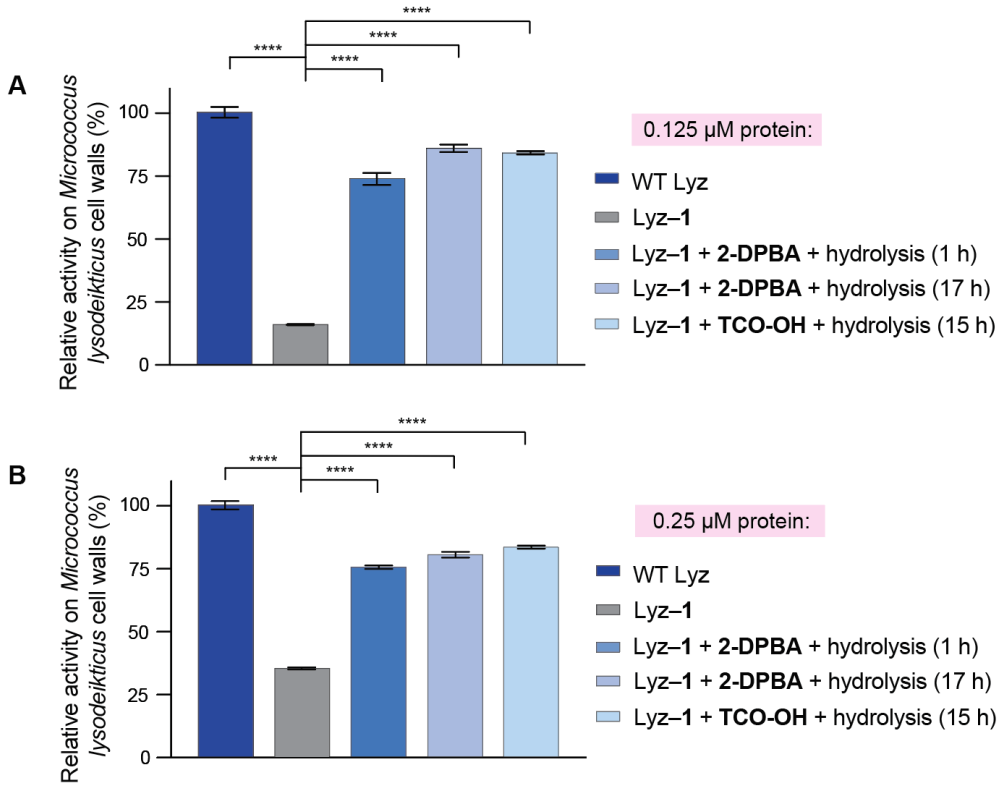

Figure S9. Relative activities of 0.125 μM (A) or 0.25-μM (B) WT Lyz, Lyz–**1**, or decaged Lyz–**1** samples on a 25 μg mL^{-1} suspension of *Micrococcus lysodeikticus* cell walls. "WT" refers to the native protein. Values are the mean ± SD (n = 3). ****p < 0.0001. Panel A is also shown in the main text as Figure 4.

7. Stability of Lyz–1 in the Presence of Pig Liver Esterase (PLE) and Lysate

7.1. M21 Cell Line and Cell Culture Conditions

The human melanoma M21 cell line[19,20] was a kind gift from Dr. Oscar Ortiz (Merck KGaA, Darmstadt, Germany). The cell line was tested negative for mycoplasma using the Lonza MycoAlert Plus kit. The M21 cell line was further authenticated by short tandem repeat profiling (STR) to validate the identity of the cell line and rule out intraspecies contamination. M21 cells were grown in sterile culture flasks in a cell culture incubator at 37 °C under CO_2 (5% v/v). Cells were counted to determine seeding density using a Countess II FL Automated Cell Counter from Thermo Fisher Scientific. To minimize genetic drift, thawed vials were used for fewer than twenty passages. M21 cells were grown in high-glucose DMEM medium (product #12100046) from Thermo Fisher Scientific supplemented with sodium bicarbonate (1.5 g L^{-1}), FBS (10% v/v), penicillin (100 U mL^{-1}), and streptomycin (100 µg mL^{-1}). The cells were passaged upon reaching 80% confluency with trypsin–EDTA (0.05%).

7.2. Bioreversibility of Lyz–1 in the Presence of PLE and Cell Lysate

Preparation of Pig Liver Esterase (PLE)

PLE from Sigma–Aldrich (Product Number: 46058, Lot # BCCD7346, specific activity of 95.7 U/mg) was dissolved in DPBS to a final concentration of 50 µM (assuming that the molecular weight of PLE is 162 kDa). 1 U corresponds to the amount of PLE that hydrolyzes 1 µmol of ethyl valerate per min at pH 8.0 and 25 °C.

Preparation of M21 Cell Lysate

M21 cells were grown to 90% confluency in T-175 flasks. Each flask was harvested with trypsin–EDTA (0.05%), washed with cold DPBS (×2), and pelleted at 1,000 g at 4 °C. The pellets were rapidly frozen with liquid N_2. Subsequently, each pellet was slowly thawed on ice and resuspended in 1 mL of cold DPBS. This freeze-thaw cycle was repeat 3 additional times. The final thawed lysates were subjected to centrifugation at 14,000*g* at 4 °C for 15 min and the resultant supernatant was aliquoted for storage at −80 °C. Total protein concentration of the supernatant was determined with a DS-11 UV–vis spectrophotometer, assuming that 1 AU = 1 mg mL^{-1} and that the average weight of a protein in the human proteome is 46 kDa. This average weight estimation was based on the reported average length of a protein in the human proteome (416 amino acids, classified in Pfam database of well-curated alignments)[21] and the average molecular weight of an amino acid (~110 Da). Each pellet resulted in a 1-mL lysate stock solution of 80 µM concentration in DPBS.

Lyz–1 Cleavage Study with PLE and M21 Cell Lysate

WT Lyz was labeled with **1** at pH 6.5 (for 7 h, as described on page S11) and buffer-exchanged into DPBS. For the PLE cleavage study, Lyz–**1** was added to a stock solution of PLE in 1:1 ratio by equivalents (30 µM final concentration of both proteins). For the lysate cleavage study, Lyz–**1** was added to a stock solution of M21 lysate in 1:1 ratio by equivalents (30 µM final concentration

of both Lyz–**1** and lysate). To access the extent of ester bond hydrolysis in DPBS, Lyz–**1** alone was diluted in DPBS to a final concentration of 30 μM. The three reactions were incubated at 37 °C with mild shaking (speed 1.5 on Titer Plate Shaker) for 4 h or 19 h. After the indicated times, the samples were analyzed by Q-TOF MS. The results of the cleavage studies are shown in Figures S10 and S11, which depict the deconvoluted mass spectra of the Lyz–**1** peak. As shown in the representative total ion chromatogram (TIC) in Figure S12B (corresponding to the data in Figure S11D), the Lyz–**1** peak did not completely co-elute with other M21 cell lysate (*e.g.,* protein) peaks. Furthermore, as shown in Figure S12D, only peaks corresponding to Lyz–**1** were distinct enough for deconvolution, likely because Lyz–**1** was the most concentrated protein in the sample. These differences in retention times and concentrations enabled the observation of clean Lyz–**1** signals (Figures S10 and S11) without interfering background from M21 cell lysate.

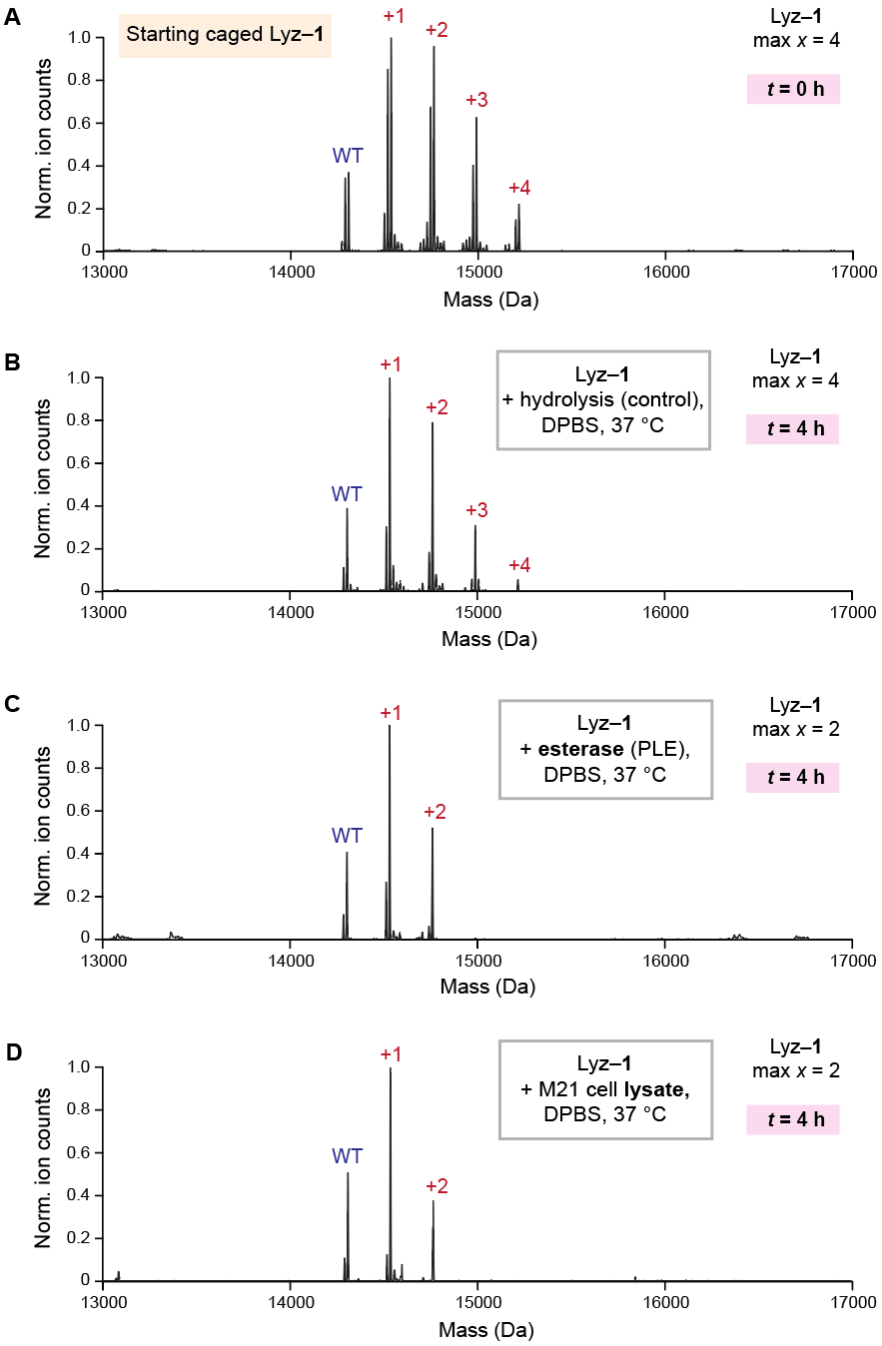

Figure S10. Deconvoluted Q-TOF mass spectra of (A) the starting Lyz–**1** conjugate, (B) Lyz–**1** subjected to hydrolysis, (C) Lyz–**1** cleaved with PLE, and (D) Lyz–**1** cleaved with M21 cell lysate in DPBS at 37 °C for 4 h. "Max *x*" refers to the maximum number of carboxyl groups esterified in Lyz–**1**. The ion intensity was normalized (norm.) so that the ordinate of the highest point is equal to 1.

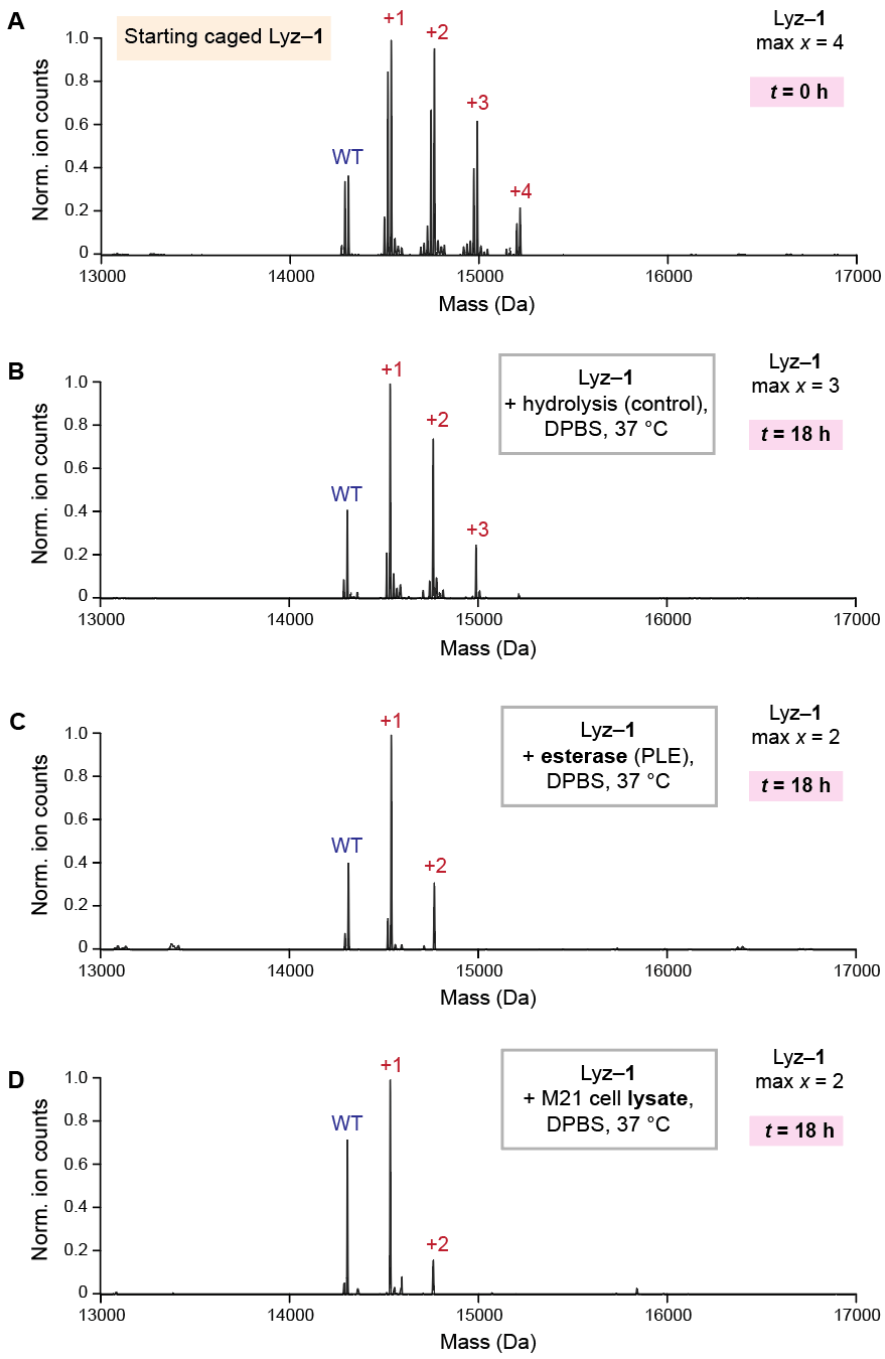

Figure S11. Deconvoluted Q-TOF mass spectra of (A) the starting caged Lyz–**1** conjugate, (B) Lyz–**1** subjected to hydrolysis for 18 h, (C) Lyz–**1** cleaved with PLE for 18 h, and (D) Lyz–**1** cleaved with M21 cell lysate in DPBS at 37 °C for 18 h. "Max *x*" refers to the maximum number of carboxyl groups esterified in Lyz–**1**. "WT" refers to the native protein. The ion intensity was normalized (norm.) so that the ordinate of the highest point is equal to 1. A truncated version of Figure S11C is depicted in Figure 5B.

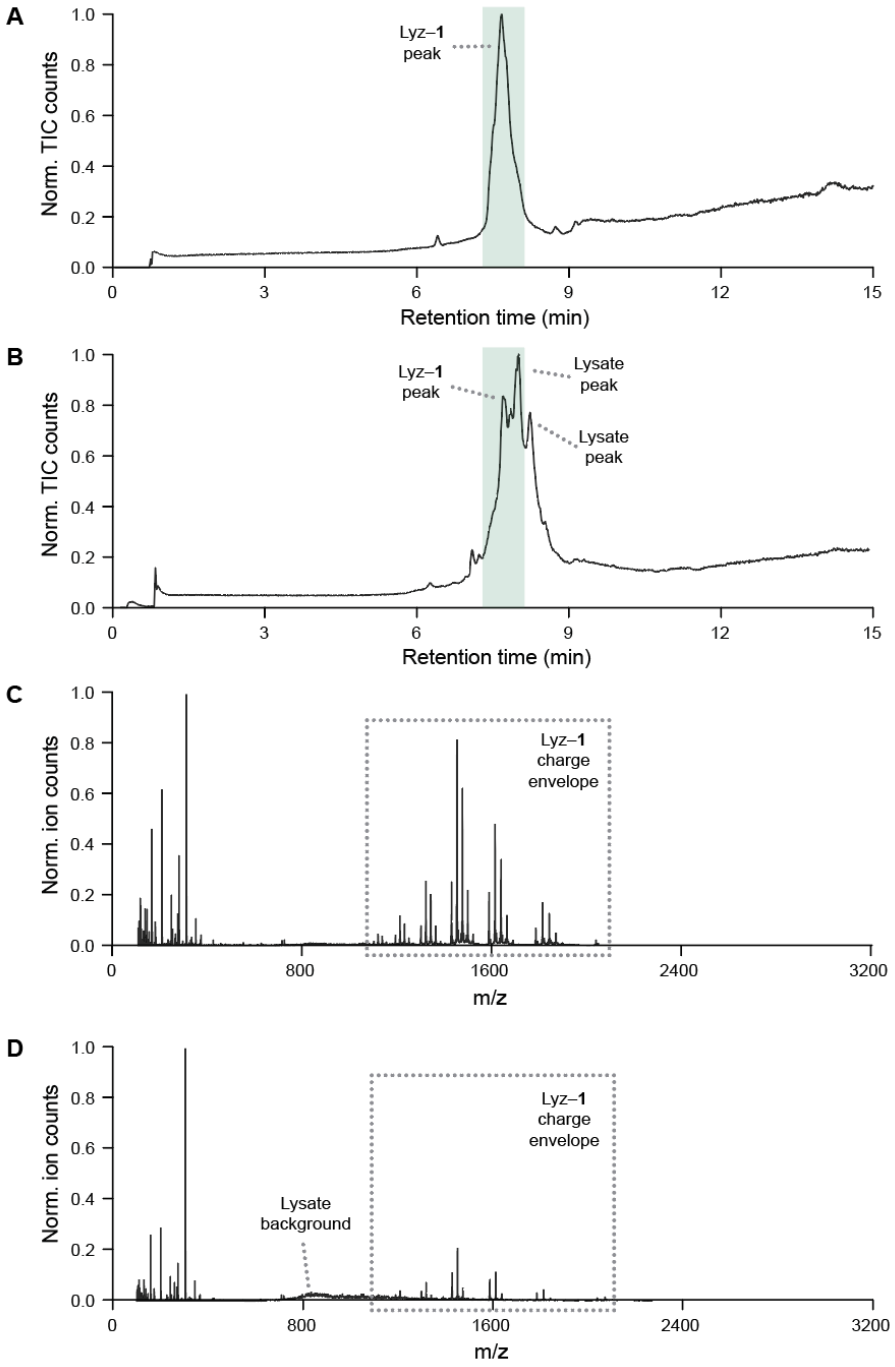

Figure S12. (A) TIC used to obtain the deconvoluted Q-TOF mass spectrum (Figure S11B) of Lyz–**1** incubated in buffer alone for 18 h. (B) TIC used to obtain the deconvoluted Q-TOF mass spectrum (Figure S11D) of Lyz–**1** incubated with M21 cell lysate for 18 h. The green rectangle in (A) and (B) were used to generate the extracted mass spectra depicted in (C) and (D), respectively. Mass spectra (C) and (D) were deconvoluted to generate Figures S11B and S11D, respectively. The TIC and the ion intensity were normalized (norm.) so that the ordinate of the highest point is equal to 1.0.

7-3. Determination of Relative k_{cat} and K_M of WT Lyz and PLE-Cleaved Lyz–1

The EnzCheck Lysozyme Assay Kit was used to determine the k_{cat} and K_M of WT Lyz and Lyz–**1**, which was cleaved with PLE for 18 h (the synthesis of this conjugate is described on pages S23–S27). Note that PLE was not removed from the sample prior to running the assay. (We attempted to remove PLE by passing the sample through an Amicon Ultra 0.5-mL Centrifugal Filter (100K), but PLE co-eluted with cleaved Lyz.) The kinetic assay was performed as described on page S21. A final concentration of 1 μM was used for WT Lyz and PLE-cleaved Lyz–**1**. The results are shown in Figure S13. The large changes in K_M could be due to the interference of PLE (a large and net negatively charged protein), which is present in the reaction mixture at the same concentration as Lyz. This could alter substrate binding by affecting the electrostatics of the overall mixture and hence the K_M. The code and datasets used are available at https://github.com/clair-gutierrez/MM_lysozyme_caging.

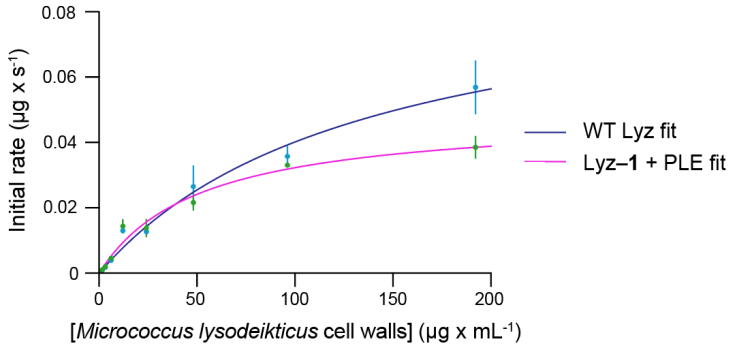

Constants	WT Lyz	Lyz–**1** + PLE	(Lyz–**1** + PLE)/WT Lyz
k_{cat} (s^{-1})	0.09 ± 0.01	0.049 ± 0.004	0.51 ± 0.12
K_M (μg x mL^{-1})	136 ± 53	51 ± 11	0.37 ± 0.17
k_{cat}/K_M (L x g^{-1} s^{-1})	0.70 ± 0.31	0.95 ± 0.22	1.37 ± 0.36

***Figure S13*. Top.** Fitted initial rates of the hydrolytic activity of WT Lyz and PLE-cleaved Lyz–**1** on *Micrococcus lysodeikticus* cell walls. "WT" refers to the native protein. **Bottom.** Table of kinetic parameters. Values are reported the mean ± SE at a 95% confidence interval (n = 4).

7-4. Intact MS Analysis of Pepsin Digests of PLE-Cleaved Lyz–1

Lyz–**1** was cleaved with PLE for 18 h as described on pages S23–S27. Note that PLE was not removed from the sample prior to intact MS analysis (we tried to remove PLE by passing the sample through an Amicon Ultra 0.5-mL Centrifugal Filter (100K), but PLE was co-eluting with cleaved Lyz, so this attempt was not successful). Denaturation and pepsin digestion of PLE-cleaved Lyz–**1** were performed as described on page S13, except, since the sample contained 1 equiv of PLE in addition to 1 equiv of cleaved Lyz, the pepsin to substrate (cleaved Lyz) ratio was changed to 1:10 w/w. Intact Q-TOF MS analysis of the sample was performed as described on page S14. Esterified residues that were not previously detected in the analysis of Lyz–**1** (synthesized at pH 6.5) digests (Figure S4) were excluded from this dataset. The results are shown in Figure S14.

```
1         10        20        30        40        50        60
KVFGRCELAAAMKRHGLDNYRGYSLGNWVCAAKFESNFNTQATNRNTDGSTDYGILQINS

          70        80        90       100       110       120
RWWCNDGRTPGSRNLCNIPCSALLSSDITASVNCAKKIVSDGNGMNAWVAWRNRCKGTDVQAWIRGCRL
```

Peptide	Esterified Residue	Peak Area	|Ppm|
GNWVCAAKF**E**S	**E35**	9.1×10^5	2.1
KF**E**SNFNT	**E35**	2.2×10^5	2.3
F**E**SN	**E35**	3.7×10^4	3.0
LGNWVCAAKF**E**	**E35**	1.8×10^4	0.8
KF**E**	**E35**	1.6×10^4	2.4
RGYSLGNWVCAAKF**E**SN	**E35**	8.2×10^3	2.7
KF**E**SNFN	**E35**	8.3×10^3	1.7
TNRNT**D**GST**D**YGILQ	D48 or D52	3.0×10^5	2.2
ST**D**YGIL	D52	2.2×10^4	0.6
T**D**YGILQINSRWWCN	D52	2.2×10^4	2.1
GST**D**YGIL	D52	1.5×10^4	2.5
T**D**YGILQINSRWW	D52	9.7×10^3	1.0
DGST**D**YGILQINS	D48 or D52	9.1×10^3	2.2
GST**D**YGILQINS	D52	7.8×10^3	0.0
PCSALLSS**DI**TASV	D87	1.1×10^5	0.7
SS**D**IT	D87	3.8×10^4	0.3
GL**D**NYRGYSLGNW	D18	3.5×10^4	1.7
MKRHGL**D**N	D18	2.2×10^4	2.5
KRHGL**D**NYRGY	D18	2.2×10^4	2.4
NT**D**G	D48	1.2×10^4	0.1

***Figure S14*. Top.** Sequence coverage of PLE-cleaved Lyz–**1** identified by Q-TOF MS post a 1-h pepsin digest. The sequence coverage in this dataset was complete. Esterified Glu35 is bolded in blue; other unambiguously esterified residues are bolded in green. **Bottom.** Caged residues are listed in the order from most abundant to least abundant in terms of peak area.

Analysis: Despite cleavage of Lyz–**1** by PLE, Glu35 is still one of the top remaining esterified residues. This dataset agrees with the kinetics analysis in Figure S13, which suggests that some active-site residues remain caged.

8. Validation of the Caging–Decaging Approach on Cytochrome *c* (Cyt *c*)

8.1. Synthesis of Caged Cyt *c* (Cyt *c*–1)

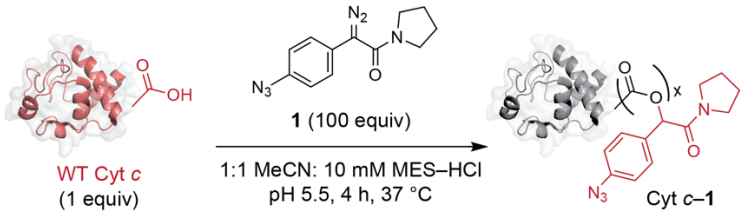

To a solution of WT Cyt *c* (500 µM, 1.0 equiv) in 10 mM MES–HCl buffer, pH 5.5, was added a solution of diazo compound **1** (50 mM, 100 equiv per protein or 6.7 equiv per carboxyl group) in MeCN (50% v/v). The reaction mixture was incubated for 4 h at 37 °C with mild shaking (speed 1.5 on Titer Plate Shaker). Subsequently, the reaction solution was buffer-exchanged into DPBS with calcium and magnesium (3×) using Amicon Ultra 0.5-mL centrifugal filters (10K). The number of ester labels on the resultant buffer-exchanged Cyt *c*–**1** conjugate was assessed by using Q-TOF MS (Figure S15).

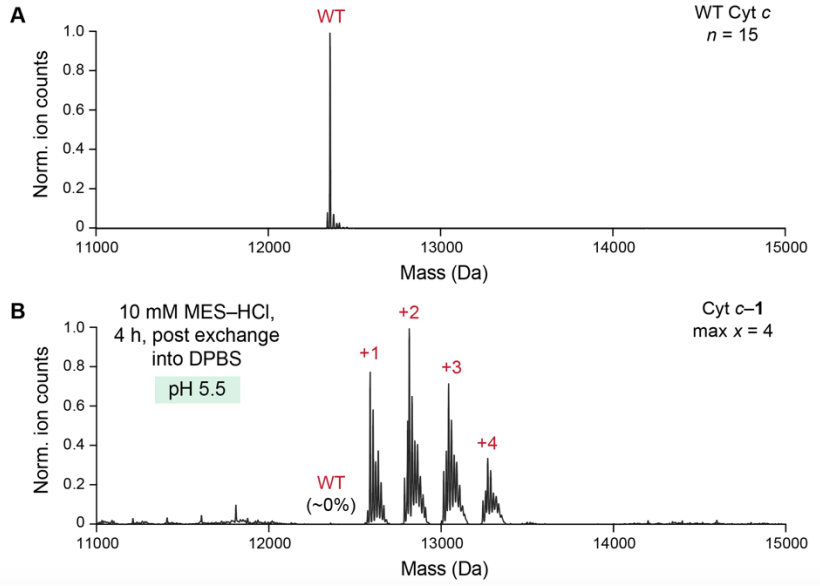

		WT Cyt *c*	+1	+2	+3	+4
Cyt *c*–**1**	Exp'd MW	12359	12587	12815	13043	13271
(+228 Da/label)	Obs'd MW	12359	12588	12816	13045	13273

***Figure S15*. Top.** Q-TOF mass spectra of (A) WT Cyt *c* and (B) Cyt *c*–**1** in DPBS. "WT" refers to the native protein. "*N*" refers to the number of carboxyl groups (including heme propionates) in WT Cyt *c*. "Max *x*" refers to the maximum number of carboxyl groups esterified in Cyt *c*–**1**. The ion intensity was normalized (norm.) so that the ordinate of the highest point is equal to 1. In addition to peaks that correspond to the expected ester labels of diazo compound **1**, we also observed adjacent peaks that correspond to a loss of 16, 18, or 19 Da, which is likely a mass spectrometry artifact. We also observed adjacent peaks that correspond to a gain of 15, 16, or 17 Da, which is likely oxidation. **Bottom.** List of expected (exp'd) and observed (obs'd) masses.

8.2. Intact MS Analysis and Absorbance Analysis (410 nm) of Glu-C Digests of Cyt *c*–1

Glu-C Digestion

See the "General Note on the Stability of Ester Bonds in Esterified Proteins" on page S13. We chose Glu-C instead of pepsin for the digestion of Cyt *c* because we wanted to obtain a smaller set of longer peptides that could be easily resolved on the column and thus be more accurately quantified via integration of absorbances at 410 nm. According to the manufacturer (Promega), Glu-C (optimal activity at pH 4–9) is a more specific enzyme than pepsin, as it only cleaves peptides on the C-terminal side of Glu and Asp residues. In contrast, pepsin has broader specificity with a preference for hydrophobic residues at P1 and P1′ positions (*e.g.,* Phe, Leu, Tyr, Trp).[17] WT Cyt *c* was labeled with **1** at pH 5.5 (for 4 h, as described on page S31) and buffer-exchanged into 100 mM MES–HCl buffer, pH 6.0. It was empirically determined that Cyt *c*–**1** does not require denaturation for efficient cleavage by Glu-C (note that WT Cyt *c* was not cleaved by Glu-C in the absence of denaturation). To initiate Glu-C-mediated cleavage, a fresh solution of Glu-C (2.6 ug, 4.7 µL in Milli-Q water) (product #V1959) from Promega was added to the solution of Cyt *c*–**1** (26 µg, 35 µL of a 60 µM solution) to achieve an enzyme:substrate w/w ratio of 1:10. The sample was incubated for 15 h at 37 °C with mild shaking (speed 1.5 on Titer Plate Shaker) and then immediately analyzed by Q-TOF MS.

Intact Q-TOF MS Analysis and Absorbance Analysis (410 nm)

The digested samples were analyzed on the Q-TOF 6530C equipped with a Poroshell 120 EC-C18 column and a 1290 Infinity II DAD FS (G7117A) as described on page S5. Because absorbance analysis was performed in addition to intact MS analysis, a 20-µM solution of digested Cyt *c* was injected into the instrument (this concentration refers to the starting amount of Cyt *c* in the sample) instead of a 2-µM solution. A gradient of 5–90% v/v MeCN (0.1% v/v formic acid) in Milli-Q water (0.1% v/v formic acid) over 21 min was used and the column was pre-heated to 30 °C. Masses of the Glu-C digests were analyzed in the program BioConfirm B.09.00 from Agilent Technologies. Peptides were searched against the sequence of "reduced" WT Cyt *c*. The Protein Digest workflow was followed with "Glu-C" defined as the cleavage enzyme. Labels of **1** were defined as variable modifications (monoisotopic delta mass: +228.101111, gain of $C_{12}H_{13}N_4O$ and loss of H, specificity for E and D residues, up to 15 modifications per protein). The heme containing two propionates was also defined as a variable modification (monoisotopic delta mass: +615.169473, gain of $C_{34}H_{32}FeN_4O_4$ and loss of H, specificity for C residues, up to 1 modification per protein). The structure of the heme *c* in Cyt *c* is shown in Figure S16. Protein digest MS match tolerance was set to ≤5 ppm and the allowed charge states were +1 and +2. Peaks with peak heights of <1000 counts were excluded from the analysis. Peptides predicted to be esterified at the C-terminal E residue were also excluded from the analysis, since Glu-C cleaves at the C-terminus of unmodified E and D residues (according to the manufacturer, Promega). Only peptides esterified at a single carboxyl group were reported as esterified for higher confidence. Peak areas were calculated by integrating the peaks in the program Qualitative Analysis B.07.00 from Agilent Technologies. The results are shown in Figure S17.

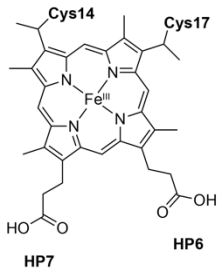

Figure S16. Structure of the heme *c* prosthetic group in Cyt *c*, which is covalently attached to the protein through two residues, Cys14 and Cys17. The two heme propionates in Cyt *c* are named heme propionate 6 (HP6, solvent-accessible, elevated pK_a of > 9) and heme propionate 7 (HP7, buried, pK_a < 4.5).[22-24] The Cyt *c* from horse heart used in this study is oxidized (according to the manufacturer, Sigma–Aldrich).

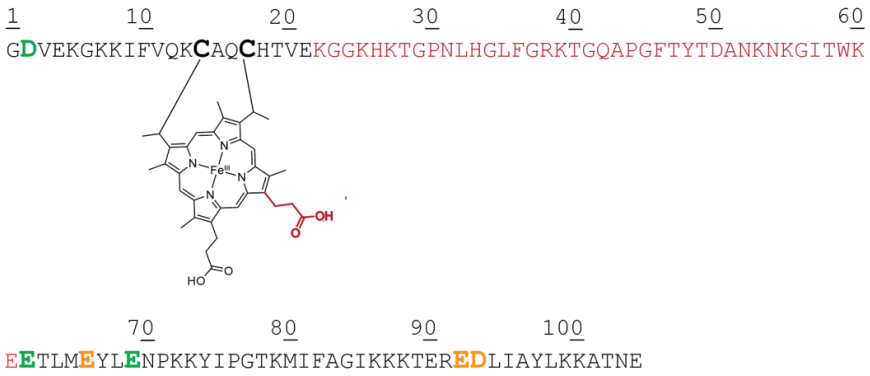

Peptide	Esterified Carboxyl Group	Peak Area	|Ppm|
KGKKIFVQKCAQCHTVE linked to **esterified** heme through 2 C residues	**HP6** or **HP7**	3.0×10^5	3.8
ETLME	E62	1.9×10^5	4.6
ETLM**E**YLE	E62 or E66	4.7×10^3	2.6
G**D**VE	D2	7.2×10^4	4.4
YL**E**NPKKYIPGTKMIFAGIKKKTE	E69	2.8×10^4	2.7
R**ED**LIAYLKKATNE	E92 or D93	1.6×10^4	4.4

Figure S17. **Top.** Sequence coverage of Cyt *c*–**1** identified by Q-TOF MS post a 15-h Glu-C digest. Portions of the sequence that were not detected are highlighted in red. An esterified heme propionate (most likely the solvent-accessible, high-pK_a HP6) is bolded in red; unambiguously esterified residues are bolded in green; possibly esterified residues are bolded in orange; Cys residues are bolded in black. **Bottom.** Esterified residues are listed in the order from most abundant to least abundant in terms of peak area.

Analysis: Overall, peptides esterified at a heme propionate are the most abundant in this dataset. The most likely propionate to be esterified out of the two is HP6, sine 1) it is the propionate with an anonymously elevated pK_a of > 9 and 2) HP6 (but not HP7) is solvent accessible.[22-24]

Absorbance-based Analysis of Glu-C Digests of Cyt c–1 at 410 nm

The heme *c* prosthetic group in Cyt *c* has an absorbance (A) maximum at 410 nm.[1] This unique property of Cyt *c* enables facile detection and quantification of native and esterified heme *c*-containing digests using a diode array detector (DAD). The intact Q-TOF MS analysis described on page S32 was thus coupled to DAD analysis at 410 nm. The resultant chromatogram of the Glu-C digest is shown in Figure S18.

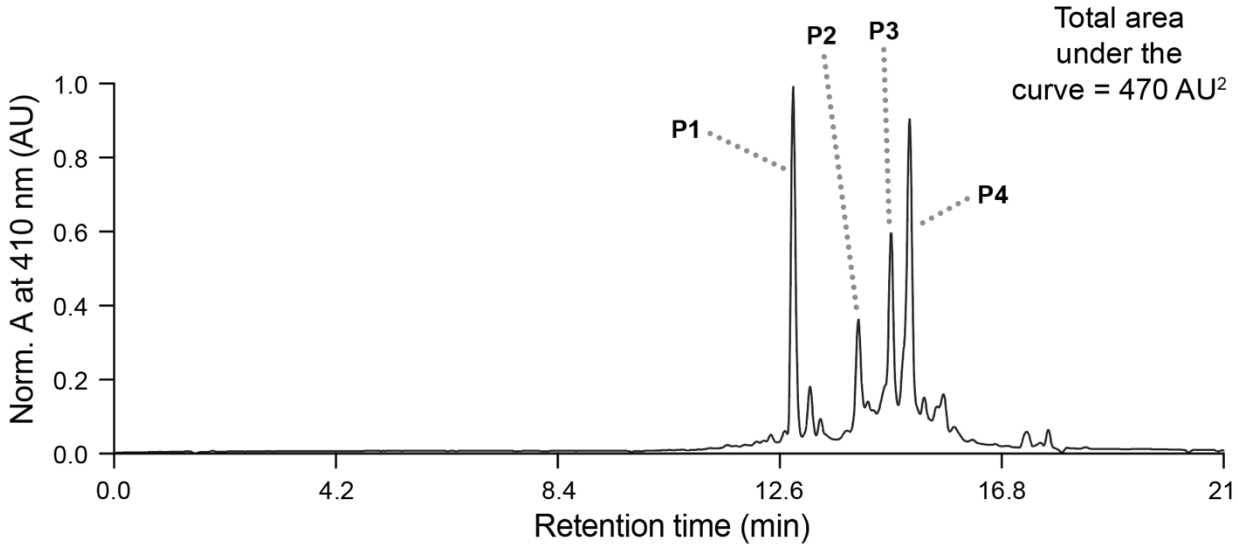

Peak	Digests Containing Heme *c*	Peak Area	|Ppm|
P4	KGKKIFVQKCAQCHTVE linked to **esterified** heme *c* through 2 C residues	108	3.8
P1	KGKKIFVQKCAQCHTVE linked to native heme *c* through 2 C residues	78.9	2.2
P3	KGKKIFVQKCAQCHTVE linked to **esterified** heme *c* through 2 C residues	75.4	3.8
P2	WT Cyt *c* (undigested)	38.1	0*

***Figure S18*. Top.** Normalized absorbance of Glu-C digests of Cyt *c*–**1** at 410 nm. The absorbance (A) was normalized (norm.) so that the ordinate of the highest point is equal to 1. **Bottom.** Identity and A corresponding to peaks **P1**–**P4**. Esterified residues are listed in the order from most abundant to least abundant in terms of peak area. *The program BioConfirm B.09.00 was not able to assign **P2**, because only peptide databases (not intact proteins) were used for matches. We deconvoluted **P2** in the software Qualitative Analysis B.07 and it output the spectrum of WT Cyt *c*.

Absorbance-based Quantification of the % of Cyt c–1 Esterified at a Heme Propionate

Minimal % of Cyt *c*–**1** esterified at a heme propionate (by concentration):

$$\frac{\sum(\text{area of all digests esterified at the heme})}{\sum(\text{area of all digests that absorb at 410 nm})} \cdot 100\% = \frac{(75.4 + 108)}{470} \cdot 100 = 39\%$$

The formula above was used to estimate the percentage of Cyt *c*–**1** esterified at a heme propionate. This formula relies on two assumptions. The first assumption is that the ratio of Cyt *c*–**1** to heme *c* is 1:1. The second assumption is that heme *c* absorbance at 410 nm scales linearly with the concentration of a given digest containing a covalently attached heme *c*. In other words, it was assumed that all heme *c*-containing digests were detected in the absorbance chromatogram shown in Figure S18. Note that the calculated value (39%) is an underestimate because a portion of esters in Cyt *c*–**1** hydrolyzed upon Cyt *c*–**1** incubation with Glu-C for 15 h at 37 °C (see page S32 for details). The background hydrolysis of a Cyt *c*–**1** control (60 µM solution in 100 mM MES–HCl buffer, pH 6.0) is shown in Figure S19 below. It is likely that esterified peptides will hydrolyze faster than an esterified protein because esters in proteins are more sterically hindered.

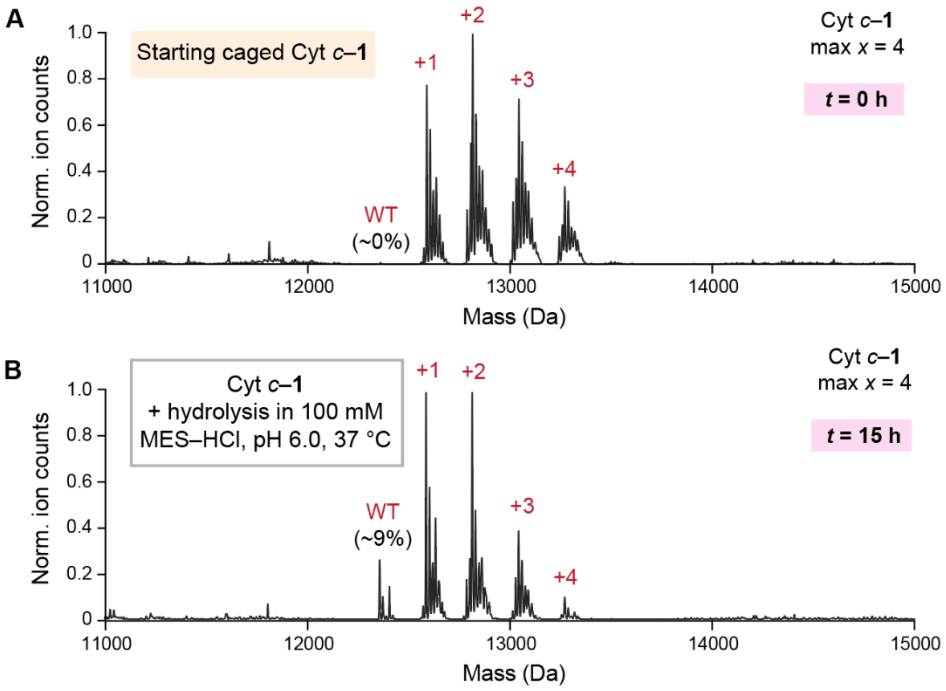

Figure S19. Q-TOF mass spectra of (A) the starting caged Cyt *c*–**1** conjugate and (B) Cyt *c*–**1** that was hydrolyzed in 100 mM MES–HCl buffer, pH 6.0, for 15 h. "Max *x*" refers to the maximum number of carboxyl groups esterified in Cyt *c*–**1**. The ion intensity was normalized (norm.) so that the ordinate of the highest point is equal to 1.

8.3. Cyt *c*–1 Decaging with 2-DPBA

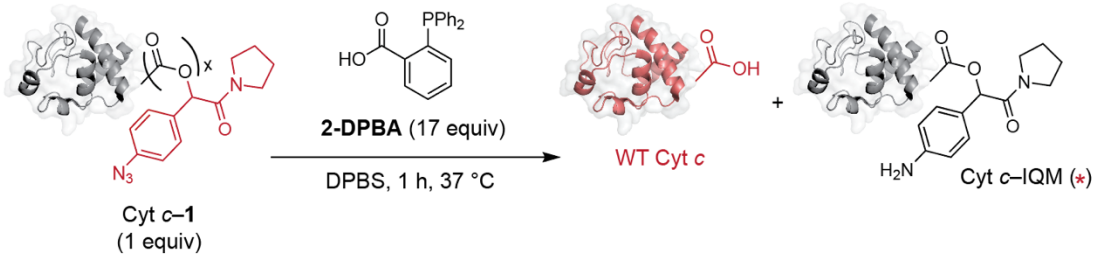

WT Cyt *c* was labeled with **1** at pH 5.5 (for 4 h, as described on page S31) and buffer-exchanged into DPBS (Figure S15). A fresh 5-mM stock solution of 2-DPBA in 1:1 MeCN/DPBS was then prepared. To initiate decaging, the 5-mM stock solution of 2-DPBA (17 equiv, 46.7 µL) was added to the solution of Cyt *c*–1 (1 equiv, 467 µL, 30 µM). The reaction mixture was incubated for 1 h at 37 °C with mild shaking (speed 1.5 on Titer Plate Shaker) and checked by Q-TOF MS (Figure S20). **Note:** Upon decaging, the oxidation state of Cyt *c* was changed from oxidized to reduced. This was inferred from two observations: (1) decaged Cyt *c* turned pink, whereas it is typically orange or dark red, and (2) a new peak appeared in the absorbance spectrum of Cyt *c* at 550 nm,[25] which indicates that the protein is reduced.

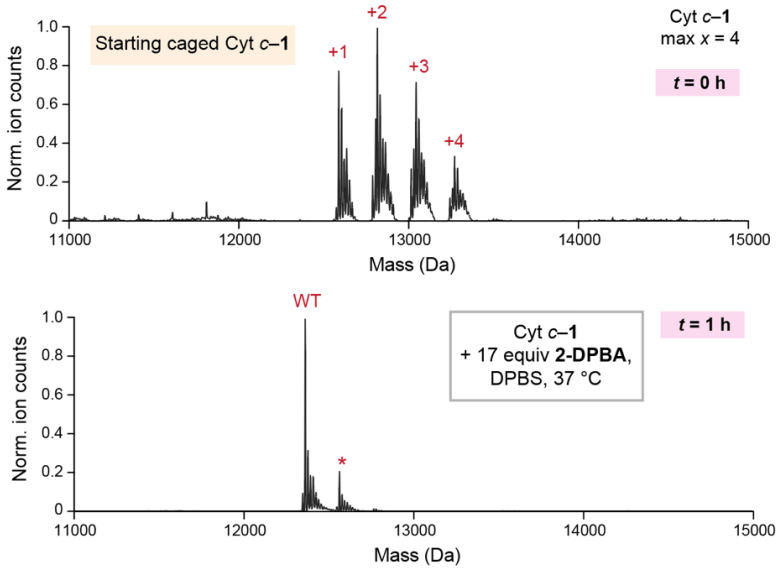

		WT Cyt *c*	+1
Cyt *c*–**IQM**	Exp'd MW	12359	12561
(+202 Da/label)	Obs'd MW	12359	12561

Figure S20. **Top.** Deconvoluted Q-TOF mass spectra of (A) the starting Cyt *c*–**1** conjugate, (B) Cyt *c*–**1** decaged with 2-DPBA. "Max *x*" refers to the maximum number of esterified carboxyl groups. The ion intensity was normalized (norm.) so that the ordinate of the highest point is equal to 1. The red asterisk refers to Cyt *c*–IQM. **Bottom.** List of expected (exp'd) and observed (obs'd) masses.

8.4. Caspase-3/7 Activation by Cyt *c* in the Cytosolic Fraction

Cytosolic Fraction Isolation from M21 Cells

Cytosolic fraction isolation from M21 cells was adapted from McStay *et al*.[26] Briefly, M21 cells were harvested, washed with cold DPBS, and pelleted by centrifugation. Pellets were resuspended in a volume of hypotonic homogenization buffer, which was 10 mM HEPES buffer, pH 7.0, containing $MgCl_2$ (5 mM), DTT (0.67 mM), and a cOmplete™ Protease Inhibitor Cocktail tablet, that was equal to the pellet volume, and the suspension was incubated on ice for 15 min. The swollen cells were lysed by passing the cell suspension 10 times through a 22-gauge needle. The homogenized cell suspension was centrifuged at 15,000g for 30 min at 4 °C to remove intact cells, heavy membranes, and nuclei. The supernatant was centrifuged again at 15,000g for 30 min at 4 °C to remove the remaining mitochondria (which contains native Cyt *c*), lysosomes, and peroxisomes. Then, the supernatant was subjected to ultracentrifugation at 100,000*g* for 1 h at 4 °C to remove the plasma membrane, microsomal fraction, and large polyribosomes. The supernatant was passed through a Spin-X Centrifugal Tube Filter (0.22-µm, cellulose acetate membrane), and its concentration was adjusted to 10 mg mL^{-1} with the homogenizing buffer. The resultant cytosolic fraction from M21 cells was aliquoted into microcentrifuge tubes and stored at −80 °C. The typical yield for 20 confluent T-75 dishes was 260 µL of cytosolic fraction (10 mg mL^{-1}).

Oxidation of Decaged Cyt c

Since WT Cyt *c* and caged Cyt *c*–**1** are oxidized, we wanted to test if the oxidation state of the decaged Cyt *c* (which is reduced post 2-DPBA addition) will impact its ability to activate caspase-3/7. Whether Cyt *c* needs to be oxidized or reduced to activate apoptosis is still an open question.[27] Therefore, we oxidized a portion of the reduced, decaged Cyt *c* prepared on page S36 as previously described in the literature.[28] Specifically, the decaged Cyt *c* (reduced) was immediately buffer-exchanged into DPBS and concentrated to 30 µM (308 µL, 1 equiv). Potassium ferricyanide was added to the solution of Cyt *c* to a final concentration of 50 µM (12 uL of a 1.25 mM stock in DPBS, 1.7 equiv). The oxidation reaction mixture was incubated for 40 min at 37 °C with mild shaking (speed 1.5 on Titer Plate Shaker). After 40 min, the decaged Cyt *c* was buffer-exchanged into Milli-Q water. It was inferred that the buffer-exchanged Cyt *c* is oxidized because (1) the solution of buffer-exchanged Cyt *c* was orange (no longer pink), and (2) the previously observed peak at 550 nm[25] (see page S36 for details) disappeared.

Immunoblot-Based Caspase-3 Cleavage Assay

WT Cyt *c*, caged Cyt *c*–**1** (synthesized as described on page S31), decaged Cyt *c*–**1** (page S36), as well as decaged and subsequently oxidized Cyt *c*–**1** (page S37) were buffer-exchanged into Milli-Q water and concentrated to 30 µM. The protocol for the assessment of caspase-3 cleavage by Cyt *c* was adapted from McStay *et al*.[26] Four 10-µL aliquots of the cytosolic fraction from M21 cells were thawed rapidly at 37 °C. To each 10-µL aliquot, 2.5 µL of a relevant Cyt *c* solution was added along with 1 µL of a 10 mM dATP solutions in Milli-Q water. The final concentration of Cyt *c* in the samples was 15 µM. The reactions were incubated at 37 °C for 30 min without shaking

(because shaking can lead to the disassembly of the apoptosome). After the indicated time, to each sample was added 13.5 µL of 2× Laemmli buffer containing 2-mercaptoethanol (5% v/v) and the samples were boiled at 95 °C for 5 min. Then, 6 µL of each sample was loaded per well of a gel and subjected to SDS–PAGE. The proteins were transferred onto a PVDF membrane using an iBlot® Gel Transfer Device. The membrane was blocked in 5% w/v non-fat dry milk in Tris-buffered saline containing Tweet 20 (0.1% v/v) (TBST) with agitation for 1 h. Subsequently, the membrane was cut and stained with either a 1:1000 dilution of a cleaved caspase-3 antibody or a 1:1000 dilution of β-actin antibody in 5% dry non-fat milk in TBST. The immunostained membranes were incubated at 4 °C overnight with agitation. After washing with TBST (×3), the membranes were stained with a 1:1000 dilution of a secondary anti-HRP-linked antibody in 5% dry non-fat milk in TBST at room temperature for 1 h with agitation. The membranes were then washed with TBST (5 × 5 min) and the blot was developed using SuperSignal West Pico PLUS Chemiluminescent Substrate according to the manufacturer's protocol. The resultant blot is shown in Figure S21. To normalize the differences between samples, an ImageJ method (version 2) was followed. Briefly, the integrated intensities of cleaved caspase-3 bands (calculated using ImageJ) and β-actin bans were calculated. Then, these integrated intensities were expressed as percentages of total caspase-3 or β-actin band intensities, respectively. The resultant caspase-3 band percentages were divided by β-actin band percentages to obtain the "relative caspase-3 activation" metric. Values were expressed as the mean ± SE of technical triplicated (n = 3) and plotted in the program Prism. SE was chosen instead of SD because immunoblot-based assays are more prone to error than are plate-based assays. The results are shown in Figure S22.

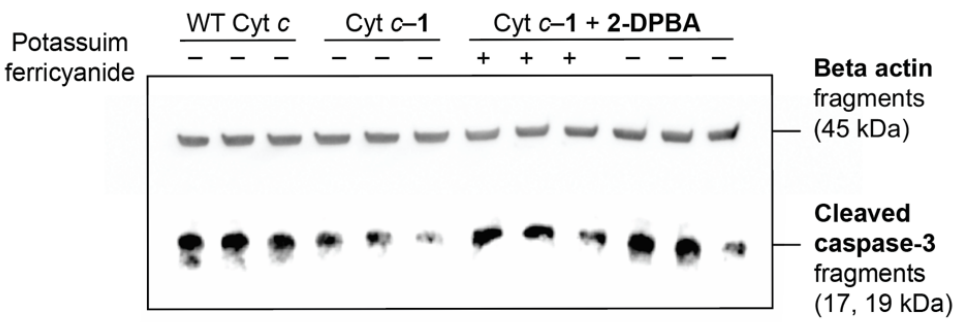

Figure S21. Immunoblot depicting caspase-3 cleavage in the cytosolic fraction from M21 cells containing 15 µM WT Cyt *c*, Cyt *c*–**1**, decaged Cyt *c*–**1**, as well as decaged and oxidized Cyt *c*–**1** (30-min time point post the addition of Cyt *c* samples to the cytosolic fraction). The three technical replicates (n = 3) are shown.

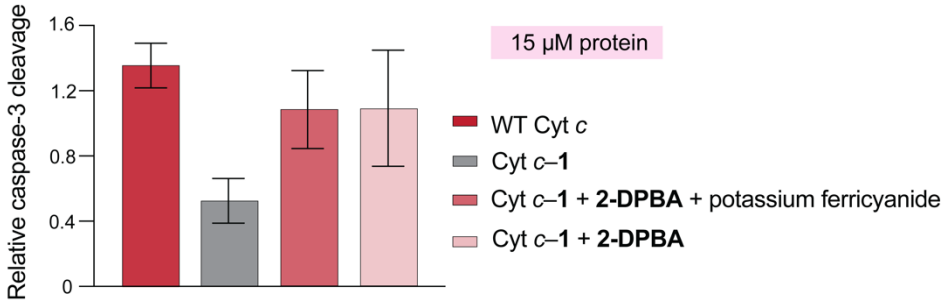

Figure S22. Relative caspase-3 cleavage in the cytosolic fraction from M21 cells containing 15 µM WT Cyt *c*, Cyt *c*–**1**, decaged Cyt *c*–**1**, as well as decaged and oxidized Cyt *c*–**1** (30-min time point post the addition of Cyt *c* samples to the cytosolic fraction). "WT" refers to the native protein. Values are the mean ± SE (n = 3).

Luminescence-Based Caspase-3/7 Activation Assay

We sought to corroborate the results of the immunoblot-based caspase-3 cleavage assay (Figures S21 and S22) using a plate-based assay, which is less subject to variability due to uneven transfer, staining, and washing steps. The Caspase-Glo® 3/7 Assay System from Promega was chosen for this purpose. WT Cyt *c*, caged Cyt *c*–**1** (synthesized as described on page S31), decaged Cyt *c*–**1** (page S36), as well as decaged and subsequently oxidized Cyt *c*–**1** (page S37) were buffer-exchanged into Milli-Q water and concentrated to 30 μM. To each 10-μL aliquot, 1 μL of Cyt *c* solution or 1 μL of Milli-Q water (as a control for baseline caspase-3/7 activity of the cytosolic fraction) was added along with 1 μL of a 10 mM dATP solutions in Milli-Q water. The final concentration of Cyt *c* in the experimental samples was 2.5 μM. The reactions were incubated at 37 °C for 20 min without shaking (shaking can lead to the disassembly of the apoptosome). In the meantime, the Caspase-Glo buffer and the luciferase substrate provided in the kit were mixed and equilibrated to room temperature (buffer A). A PIPES-based buffer (20 mM PIPES–NaOH, 100 mM NaCl, 1 mM EDTA, 10% sucrose) was also prepared and equilibrated to room temperature (buffer B). At the end of the 20 min, each aliquot containing the cytosolic fraction was diluted with 300 μL of a solution containing premixed buffer A and buffer B in 1:1 ratio. The contents of the diluted reaction were mixed and added in 20-μL aliquots to a white, 384-well, flat-bottom plate (technical triplicates, $n = 4$). Luminescence was recorded using an infinite M1000 plate reader from Tecan. The average luminescence intensity of the baseline control was subtracted from the average intensity of the samples. A sample end point (50 s) measurement is plotted in Figure S23.

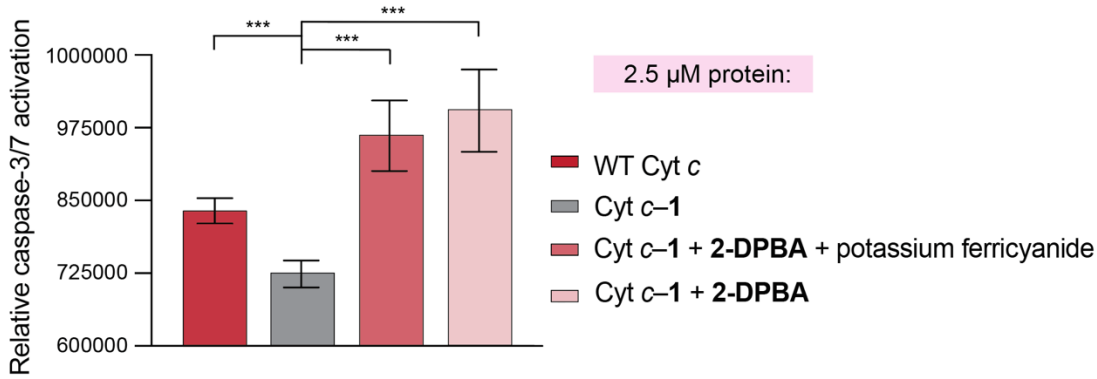

Figure S23. Relative caspase-3/7 activation in the cytosolic fraction from M21 cells containing 15 μM WT Cyt *c*, Cyt *c*–**1**, decaged Cyt *c*–**1**, as well as decaged and reduced Cyt *c*–**1** (50-s time point post addition of the luciferase-containing buffer, 20-min time point post the addition of Cyt *c* samples to the cytosolic fraction). "WT" refers to the native protein. Values are the mean ± SD ($n = 4$). ***$p < 0.001$.

Analysis: The immunoblot- and luciferin-based assays indicate that (1) the esterification of the heme propionate lowers the ability of Cyt *c* to activate caspases (a proxy for apoptosis),[29] and (2) decaging leads to an increase in activity relative to the caged conjugate. The differences between the results of the two assays can be rationalized by the fact that one measures the *total*

concentration of *caspase-3* cleaved over 30 min, whereas the other measures the *activity* of *caspase-3/7* at a specific time point (in this case, 20 min).

9. Validation of the Caging–Decaging Approach on HIV-1 Protease (HIVPR)

9.1. Expression of HIVPR with 5 Stabilizing Mutations

Production

HIVPR was expressed with 5 stabilizing mutations (Q7K, L33I, L63I, C67A and C95A) in *E. coli* as described previously with some minor changes.[30] These mutations remove the risk of cysteine oxidation and restrict autoproteolysis, though not fully.[31-32] The expression plasmid was prepared as described previously[33] and transformed into BL21 (DE3) cells. A 15-mL starter culture was taken from a single colony and grown overnight in Luria–Bertani (LB) medium with ampicillin at 37 °C (constant shaking at 250 rpm). Full scale 1-L cultures were initiated at a starting OD_{600} of 0.05 from the starter culture and grown at 37 °C in LB with ampicillin (constant shaking at 250 rpm). Cultures were induced with IPTG (final concentration: 1 mM) when they reached an OD_{600} of 1.0–1.5 and grown at 37 °C for an additional 3 h. Cultures were then pelleted at 6,000g for 15 min at 4 °C, and pellets were stored at −80 °C until lysis.

Purification

Cell pellets containing HIVPR were resuspended in 20 mM Tris–HCl buffer, pH 7.4, containing 1 mM EDTA (1 g of wet pellet per 10 mL of buffer). Cells were lysed via sonication at 4 °C via pulses of 10 s followed by 30 s of rest for 10 min. Inclusion bodies were isolated via centrifugation at 10,500g at 4 °C for 2 h. The resultant inclusion bodies were then resuspended in 20 mM Tris, 8 M urea, pH 8.0, for 1 h at room temperature (1 g of wet pellet pre-lysis per 2 mL of buffer). Insoluble material was then removed centrifugation at 30,000*g* for 1 h at 4 °C. The resultant supernatant was passed through a 0.45-μm filter. Purification was done using an Akta Pure FPLC system. The solubilized inclusion bodies were first passed through a HiTrap HP Q column to remove anionic contaminants. The resultant flow-through was diluted 20-fold using refolding buffer, which was 50 mM sodium acetate buffer, pH 5.0, containing 100 mM NaCl, 5% v/v propylene glycol, and 10% v/v glycerol. In this work, ethylene glycol (which was used previously)[30] was substituted with the more environmentally friendly propylene glycol. This substitution had a negligible effect on protease folding. The folded protease was concentrated using a stirred-cell concentrator from Amicon via a 10 kDa molecular-weight cutoff membrane before it was applied to a Superdex HiLoad 26/600 75 pg gel filtration column. Fractions containing the protease were checked by QTOF MS, concentrated, and buffer-exchanged into 2 mM MES–HCl buffer, pH 6.0, containing 2 mM NaCl. Aliquots were flash frozen in liquid N_2 and stored at −80 °C. A yield of 200 μg of HIVPR was obtained per liter of culture.

9.2. Synthesis of Caged HIVPR (HIVPR-1)

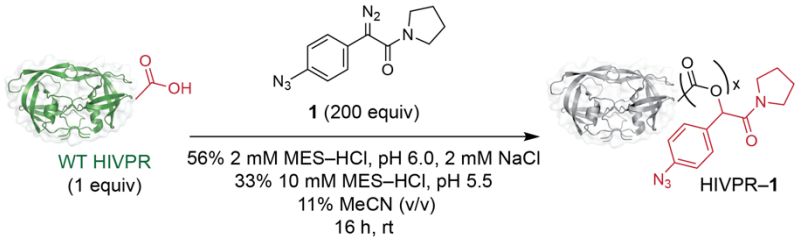

The solution of WT HIVPR (6.25 µL, 96 µM, 1.0 equiv) in 2 mM MES–HCl buffer, pH 6.0, containing NaCl (2 mM) was diluted with 3.75 µL of 10 mM MES–HCl buffer, pH 5.5. To the diluted solution was added a solution of diazo compound **1** (1.2 µL, 100 mM, 200 equiv per protein or 22 equiv per carboxyl group) in MeCN (11% v/v). The reaction mixture was incubated for 16 h at room temperature with mild shaking (speed 1.5 on Titer Plate Shaker). Where possible, we avoided prolonged incubations at 37 °C because HIVPR (even our stabilized variant)[31,32] has some propensity to autodegradation.[34] Subsequently, the reaction mixture was buffer-exchanged (3×) into 2 mM MES–HCl buffer, pH 6.0, containing NaCl (2 mM) using Amicon Ultra 0.5-mL centrifugal filters (10K). The number of ester labels on the resultant buffer-exchanged HIVPR–**1** conjugate was assessed with Q-TOF MS (Figure S24). Larger amounts of HIVPR–**1** were accessed via multiple esterification reactions rather than scaling-up the procedure outlined above.

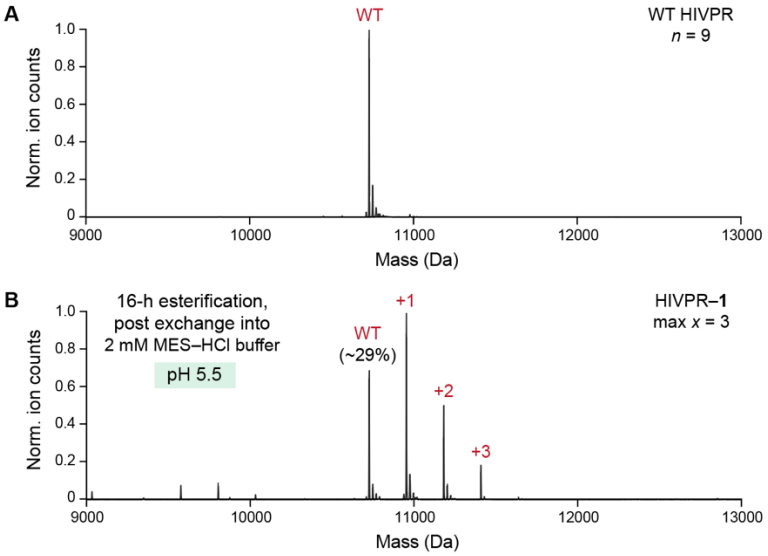

		WT HIVPR	+1	+2	+3
HIVPR–**1**	Exp'd MW	10729	10957	11185	11413
(+228 Da/label)	Obs'd MW	10729	10957	11185	11413

***Figure S24*. Top.** Q-TOF mass spectra of (A) WT HIVPR and (B) HIVPR–**1** in 2 mM MES–HCl buffer, pH 6.0, containing 2 mM NaCl. "WT" refers to the native protein. "*N*" refers to the number of carboxyl groups in WT HIVPR. "Max *x*" refers to the maximum number of carboxyl groups esterified in HIVPR–**1**. The ion intensity was normalized (norm.) so that the ordinate of the highest point is equal to 1. **Bottom.** List of expected (exp'd) and observed (obs'd) masses.

Note on the Dimerization State of HIVPR

WT HIVPR is an obligate homodimer (K_d for the dimer dissociation is 23 pM).[35] Although we have not experimentally tested if caged HIVPR–**1** remains a dimer, all manipulations of the caged protein were carried out at much higher concentrations than 23 pM. Furth, a study by Hecht and coworkers[36] showed that HIVPR dimerizes even with a bulky nitrobenzyl ester on the D25′ side chain. Based on these considerations, we depicted HIVPR–**1** as a dimer on pages S42 and S45–S46.

9.3. Intact MS Analysis of Pepsin Digests of HIVPR–1

Denaturation and Pepsin Digestion

See the "General Note on the Stability of Ester Bonds in Esterified Proteins" on page S13. WT HIVPR was labeled with **1** at pH 5.5 (for 16 h, as described on page S42) and buffer-exchanged into 2 mM MES–HCl buffer, pH 6.0, containing 2 mM NaCl. The digestion of HIVPR–**1** by pepsin was performed as described on page S13 with minor modifications. HIVPR–**1** (10 µg, 30 µL, 32 µM) was diluted with 69 µL of Milli-Q water and 1 µL of Milli-Q water containing 10% v/v formic acid. A fresh stock solution of 0.01 mg mL^{-1} pepsin (product #V1959) from Promega was prepared in Milli-Q water containing 0.1% v/v formic acid. This pepsin stock solution (0.5 µg, 50 µL) was then added to the solution of HIVPR–**1** (100 µL) to achieve a pepsin:substrate w/w ratio of 1:20. The samples were incubated for 30 min at 37 °C with mild shaking (speed 1.5 on Titer Plate Shaker). After the indicated time, the sample was immediately analyzed by Q-TOF MS.

Intact Q-TOF MS Analysis

Intact Q-TOF MS analysis was performed exactly as described on page S14, except for the following modifications: 1) peptides were searched against the sequence of "non-reduced" WT HIVPR, 2) a gradient of 5–90% v/v MeCN (0.1% v/v formic acid) in Milli-Q water (0.1% v/v formic acid) over 21 min was used, and 3) the column was pre-heated to 30 °C. The results are shown in Figure S25.

```
1         10        20        30        40        50        60
PQITLWKRPLVTIKIGGQLKEALLDTGADDTVIEEMSLPGRWKPKMIGGIGGFIKVRQYD

          70        80        90        99
QIIIEIAGHKAIGTVLVGPTPVNIIGRNLLTQIGATLNF
```

Peptide	Esterified Residue	Peak Area	|Ppm|
GQLK**E**ALL**D**	E21 or **D25′**	5.6×10^4	2.9
IKIGGQLK**E**ALL**D**TGA**DD**TVI**EE**	E21 or **D25′** or D29 or D30 or E34 or E35	1.9×10^4	2.7
IGGQLK**E**ALL**D**T	E21 or **D25′**	1.2×10^4	1.4
DTGA**DD**TVI**EE**MSLPGRWKPKM	**D25′** or D29 or D30 or E34 or E35	5.0×10^3	2.7
DTGA**D**	**D25′** or D29	1.6×10^3	0.7
KMIGGIGGFIKVRQY**D**QIII**E**	D60 or E65	2.1×10^4	2.3
QIII**E**IAGHKAIGT	E65	1.6×10^4	1.0
III**E**	E65	1.1×10^4	2.7
FIKVRQY**D**QIII**E**IAGHKAI	D60 or E65	8.5×10^3	0.9
VRQY**D**QIII**E**	D60 or E65	4.3×10^3	1.3
GA**DD**TVI**EE**MSLPGRWKPKM	D29 or D30 or E34 or E35	8.6×10^3	0.2
GQLK**E**AL	E21	5.6×10^3	1.1

Figure S25. **Top.** Sequence coverage of HIVPR–**1** identified by Q-TOF MS post a 30-min pepsin digest. The sequence coverage in this dataset was complete. Unambiguously esterified residues are bolded in green; possibly esterified residues are bolded in orange. **Bottom.** Esterified residues are listed in the order from most abundant to least abundant in terms of peak area.

Analysis: Overall, the peptide GQLKEALLD esterified at either D25′ (which is an active-site residue with an elevated pK_a, the range of reported values is 4.9–7.3)[37-41] or E21 was the most abundant in this dataset. Despite the broad specificity of pepsin, we were not able to detect shorter esterified peptides in which D25′ was the sole carboxyl group. Nevertheless, these results support the possibility that D25′ in WT HIVPR was esterified.

9.4 HIVPR-1 Decaging with 2-DPBA

Decaging Procedure A

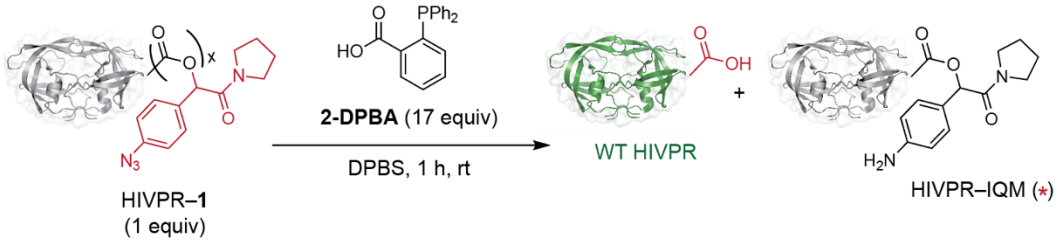

WT HIVPR was labeled with diazo compound **1** at pH 5.5 for 16 h, as described on page S42, and buffer-exchanged into DPBS (Figure S24). A fresh 5-mM stock solution of 2-DPBA in 1:1 MeCN/DPBS was then prepared. To initiate decaging, the 5-mM stock solution of 2-DPBA (17 equiv, 7.3 µL) was added to the solution of HIVPR–**1** (1 equiv, 73 µL, 29 µM). The reaction mixture was incubated for 1 h at room temperature with mild shaking (speed 1.5 on Titer Plate Shaker) and then buffer-exchanged (3×) into 2 mM MES–HCl buffer, pH 6.0, containing NaCl (2 mM) using Amicon Ultra 0.5-mL centrifugal filters (10K). The resultant sample, "HIVPR–**1** + **2-DPBA** (buffer-exchanged)," was analyzed by using Q-TOF MS (Figure S26).

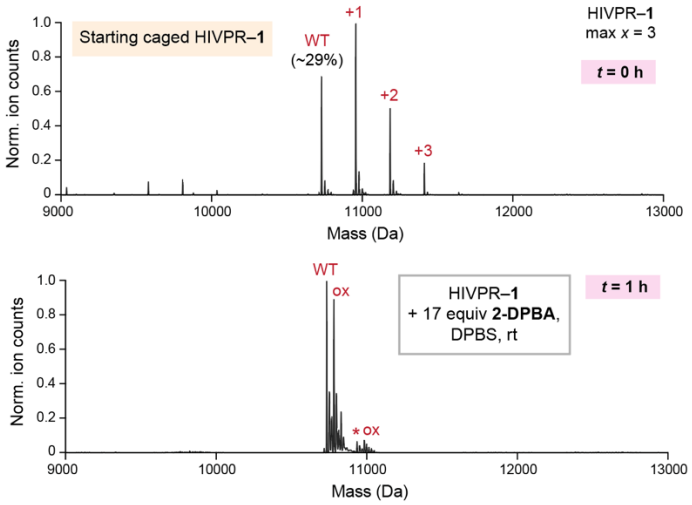

		WT HIVPR	+1 IQM
HIVPR–**IQM** (+202 Da/label)	Exp'd MW	10729	10931
	Obs'd MW	10729	10931
Oxidation (ox) (+48 Da)	Exp'd MW	10777	10979
	Obs'd MW	10777	10979

Figure S26. **Top.** Deconvoluted Q-TOF mass spectra of (A) the starting HIVPR–**1** conjugate, (B) HIVPR–**1** decaged with 2-DPBA. "Max *x*" refers to the maximum number of esterified carboxyl groups. The ion intensity was normalized (norm.) so that the ordinate of the highest point is equal to 1. The red asterisk refers to HIVPR–IQM. The observed oxidation, "ox," might be an MS artifact. **Bottom.** List of expected (exp'd) and observed (obs'd) masses.

Decaging Procedure B

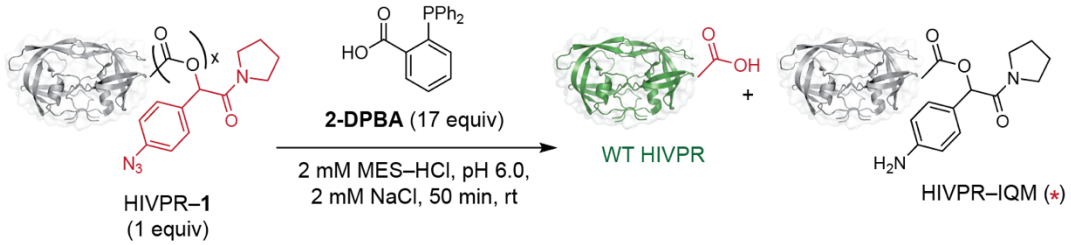

WT HIVPR was labeled with diazo compounds **1** at pH 5.5 for 16 h, as described on page S42, and buffer-exchanged into 2 mM MES–HCl buffer, pH 6.0, containing NaCl (2 mM) (Figure S24). A fresh 5-mM stock solution of 2-DPBA in 1:1 MeCN/DPBS was then prepared. To initiate decaging, the 5-mM stock solution of 2-DPBA (17 equiv, 2 µL) was added to the solution of HIVPR–**1** (1 equiv, 20 µL, 29 µM). The reaction mixture was incubated for 50 min at room temperature with mild shaking (speed 1.5 on Titer Plate Shaker) and immediately used in the FRET assay described on page S47–S48. This sample was referred to as "HIVPR–**1** + **2-DPBA**." Note that the decaging reaction mixture was purposefully not buffer-exchanged using Amicon Ultra 0.5-mL centrifugal filters (10K).

9.5. FRET Substrate Cleavage by HIVPR

Sample Preparation

WT HIVPR and HIVPR–**1** (synthesized as described on page S42) were buffer-exchanged into 2 mM MES–HCl buffer, pH 6.0, containing NaCl (2 mM). The sample "HIVPR–**1** + **2-DPBA** (buffer-exchanged)" was synthesized using the Decaging Procedure A described on page S45 and buffer-exchanged into 2 mM MES–HCl buffer, pH 6.0. The sample "HIVPR–**1** + **2-DPBA**" was synthesized using the Decaging Procedure B described on page S46 and used in the FRET assay directly.

FRET Assay with a Peptide Substrate

To determine the activity of HIVPR, a FRET-based assay was used (the results are shown in Figure S27). For expediency, we used a commercially available peptide substrate instead of the more sensitive one reported by Winsdor and Raines.[33] The peptide had the following sequence: DABCYL-GABA-Ser-Gln-Asn-Tyr-Pro-Ile-Val-Gln-EDANS (Anaspec). A 1-mM stock solution of the substrate was prepared in MeCN. The proteins and the substrate were combined to a final concentration of 0.4 μM and 10 μM, respectively, in 2 mM MES–HCl buffer, pH 6.0, containing NaCl (2 mM) and MeCN (1%) (final volume: 100 μL). HIVPR exists as a dimer with a K_d = 23 pM,[35] so at the concentration used here it was assumed most of the protease would be in the dimer form. Assays were performed in black 96-well half area plates with four technical replicates. Reads were performed on a Tecan Spark plate reader with an excitation at 340 nm and emission at 490 nm for 1 h at room temperature. Following the reactions, the background relative fluorescence (RFU) was subtracted from each point based on conditions with no protease to obtain $I_{max} - I_0$. Least-squares linear regression on the linear portion of each reaction was used to calculate the uncalibrated initial rate, $d(I_{max} - I_0)/dt$. From these initial rates the relative reaction rates were derived as shown below. Based on the previously reported literature values,[30] we assumed that $K_M \approx 103$ μM for catalysis of the cleavage of the peptide used in this study by WT HIVPR. Because the concentration of the peptide in our assays was 10 μM, the relationship [S] << K_M held true. Hence, Eq 1 was combined with Eq 2 (page S12) in the following approximation:

$$v = \frac{\mathrm{d[P]}}{\mathrm{d}t} = \frac{\mathrm{d}(I-I_0)}{\mathrm{d}t}\frac{[\mathrm{S_0}]}{(I_{\mathrm{max}}-I_0)} = \frac{k_{\mathrm{cat}}[\mathrm{E}][\mathrm{S_0}]}{K_\mathrm{M} + [\mathrm{S_0}]} \approx \frac{k_{\mathrm{cat}}[\mathrm{E}][\mathrm{S_0}]}{K_\mathrm{M}} \tag{4}$$

resulting in

$$\frac{\mathrm{d}(I-I_0)}{\mathrm{d}t} \approx \frac{k_{\mathrm{cat}}[\mathrm{E}](I_{\mathrm{max}}-I_0)}{K_\mathrm{M}} \tag{5}$$

To obtain the relative rate, we can then divide Eq 5 by the rate of WT HIVPR. The following ratio is then obtained as the enzyme concentration and $I_{max} - I_0$ are constants:

$$\text{relative rate} = \frac{k_{\text{cat}}/K_{\text{M}}}{\{k_{\text{cat}}/K_{\text{M}}\}_{\text{WT}}} \quad (6)$$

Therefore, the relative rates shown in Figure S27 illustrate the relative apparent $k_{\text{cat}}/K_{\text{M}}$ for a given protein or protein conjugate. Because Eq 5 is sensitive to input enzyme concentrations and HIVPR has been reported to be at a risk of auto-proteolysis, it was critical to use the BCA assay (rather than extinction coefficient-based measurements) to determine final concentrations of the HIVPR samples immediately before the assay was run.

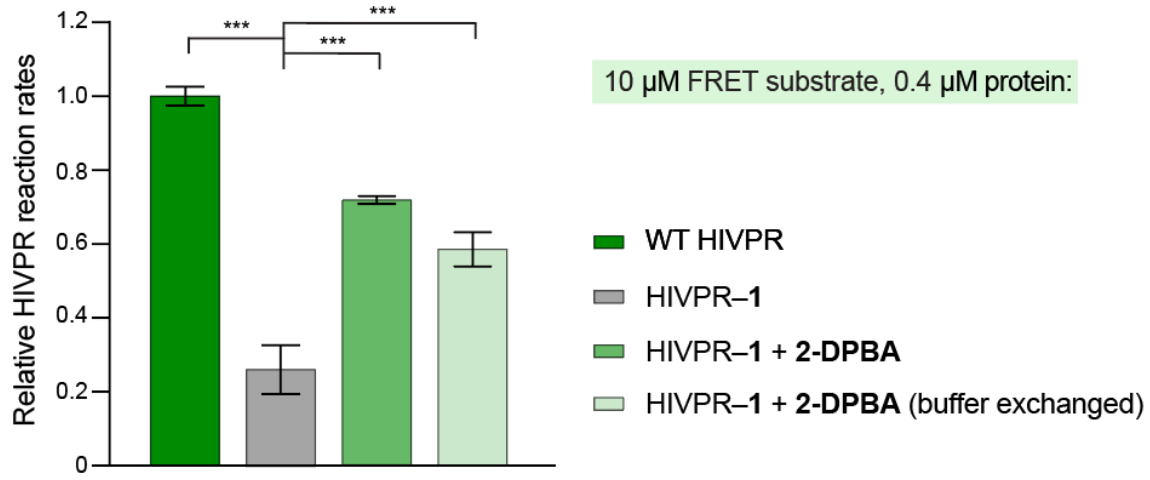

Figure S27. Caging of WT HIVPR results in decreased relative apparent k_{cat}/K_M, which is restored upon decaging with 2-DPBA. Values are the mean ± SD (n = 4). ***$p < 0.001$.

Analysis: Based on analysis of the initial rates, HIVPR–**1** was about 4-fold less active than WT HIVPR, which supports the hypothesis that the active site residue, D25′, was caged. The relative $k_{\text{cat}}/K_{\text{M}}$ of HIVPR–**1** (0.26 ± 0.07) roughly corresponded to the remaining amount of WT protein (~29%) in the Q-TOF MS spectrum of HIVPR–**1** (Figure S24) supporting that caging of HIVPR completely inactivates the protein. Note that we have not conducted the full Michaelis-Menten analysis here due to (1) limiting amounts of HIVPR, and (2) the necessity for considering dimer formation in the kinetics (an accurate analysis would have required additional reactions). Therefore, the apparent $k_{\text{cat}}/K_{\text{M}}$ with the above approximations, which is also sensitive to interruption in dimer formation and changes in K_{M}, was used as a proxy for k_{cat}. Following decaging, the activity of HIVPR was restored, albeit incompletely. This incomplete reactivation could be due to the oxidation of HIVPR post-decaging, some auto-proteolysis, or a disruption of the HIVPR dimer.

Comments on dimerization and activity of HIVPR–1

It is important to note the limitations of the HIVPR assays and our assumptions. First, the general $k_{\text{cat}}/K_{\text{M}}$ used is not nearly as useful as k_{cat} for determining whether the active site is caged,

particularly for a dimer. Yet, with the experimental limitations mentioned above, it is still a helpful metric to measure general reaction rate (with the caveat that it is less representative of active site-specific caging). Second, based on intact MS analysis of digested HIVPR–**1** (Figure S25), there is a possibility that E21 was esterified instead of D25′. Notably, unlike D25′, E21 is not at the dimer interface nor is it involved in catalysis.[42] Third, when a dimer is caged, there are three possible resultant complexes: WT·WT, WT·Caged, and Caged·Caged. The activities and dissociation constants of each of these complexes are not necessarily straightforward or easy to distinguish. If 29% of the protein remains uncaged (as suggested by Figure S24), then, by a purely random pairing, we would expect 8.4% of the complexes to be WT·WT, 41.2% to be WT·Caged, and 50.4% to be Caged·Caged. If only the WT·WT complex is active, then we would expect the activity of HIVPR–**1** to be 8.4% of the activity of the WT protein, not 26% (as seen in Figure S27). The "random pairing" scenario is, however, unlikely because esterification of D25′ (or another residue) may raise the K_d of WT·Caged and Caged·Caged dimers relative to that of the WT·WT dimer. For example, it has been shown that even a conservative D25N mutation increases the K_d of the dimer to ~1 μM.[43] If we assume (1) that the WT·Caged complex has a K_d that is between that of the WT·WT and Caged·Caged complexes, and (2) conservatively give the Caged·Caged complex a K_d of 1 μM, then although at some conditions the caged protease will exist as a dimer, the WT dimer will be more favored, as shown in Figure S28. For the enzymatic assays, the WT dimer accounts for ~20% of the total enzyme in HIVPR-**1**, which is close to the value obtained for its k_{cat}/K_M (0.26 ± 0.07) and is likely a low estimate. Overall, our assumption that the amount of WT remaining is mostly in the active dimer formation is likely reasonable and is consistent with active-site caging, supporting that caging disables the protease.

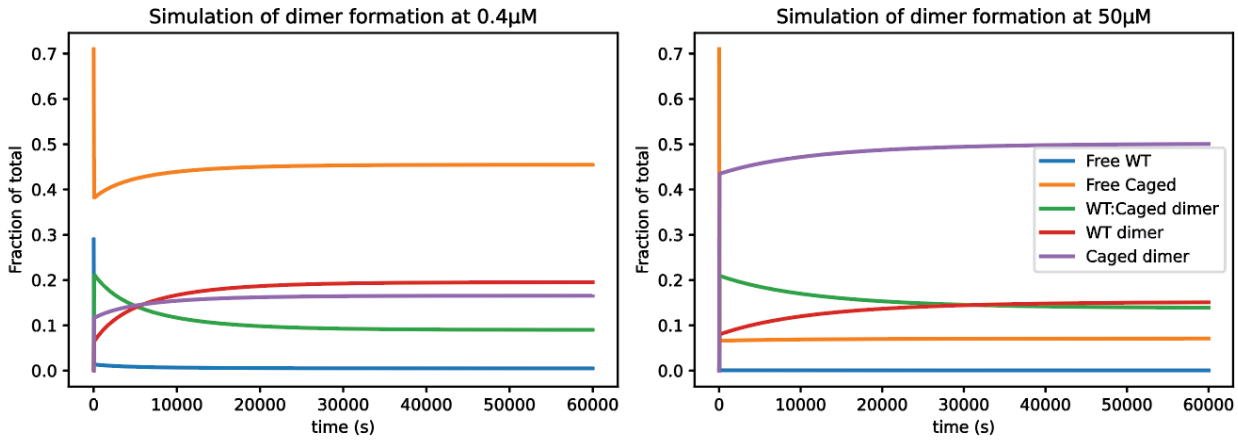

Figure S28. Simulation of dimer formation between different species assuming conservatively that the K_d of the WT·WT dimer is 100 pM, the K_d of the WT·Caged dimer is 10 nM, and the K_d of Caged·Caged dimer is 1 μM, and an association rate constant of 0.4 μM^{-1} s^{-1} (as reported previously[44]). The code, assumptions, equilibrium equations, and differential equations used for modeling can be found at https://github.com/clair-gutierrez/MM_lysozyme_caging. **Left.** Concentration used for catalytic assays. **Right.** Concentration of protease used for esterification.

10. NMR Spectra

^{1}H NMR (400 MHz) spectrum of **S1** in $CDCl_3$

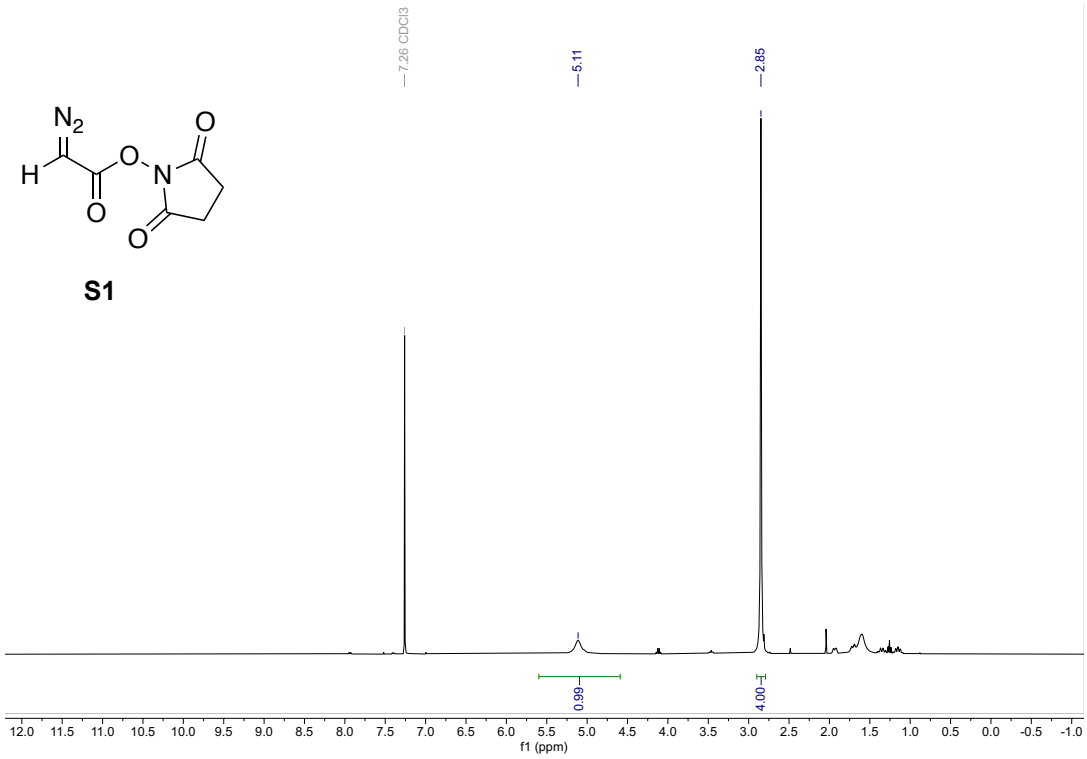

S1

^{1}H NMR (500 MHz) spectrum of **S2** in $CDCl_3$

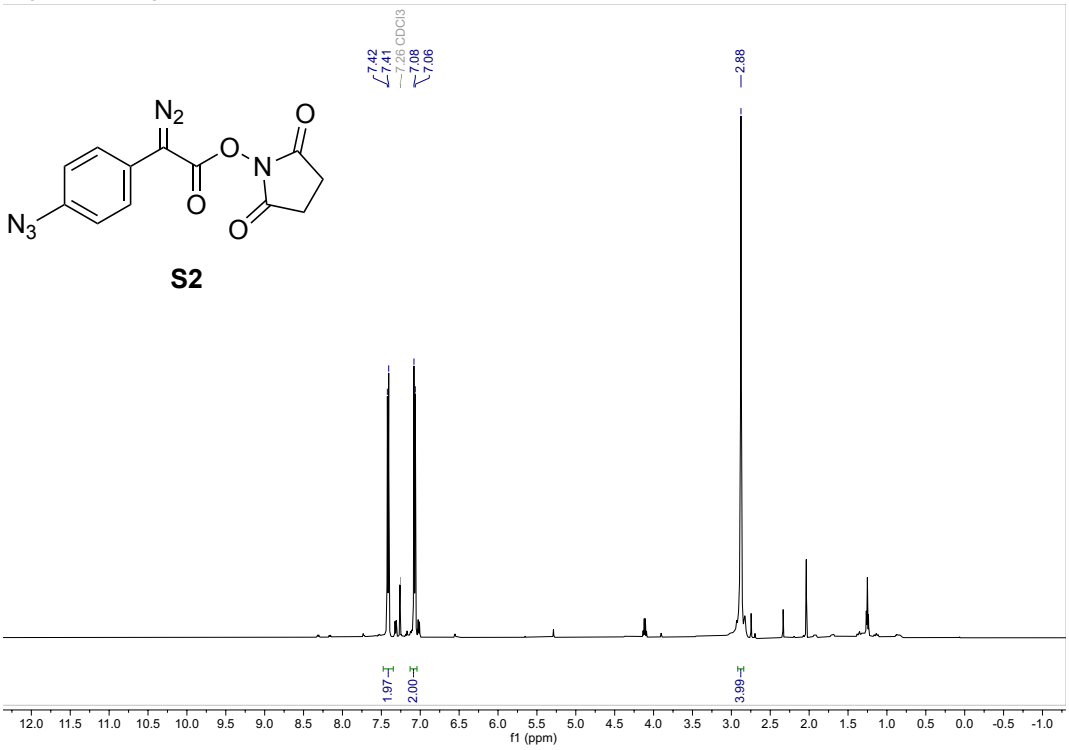

S2

^{13}C NMR (126 MHz) spectrum of **S2** in $CDCl_3$

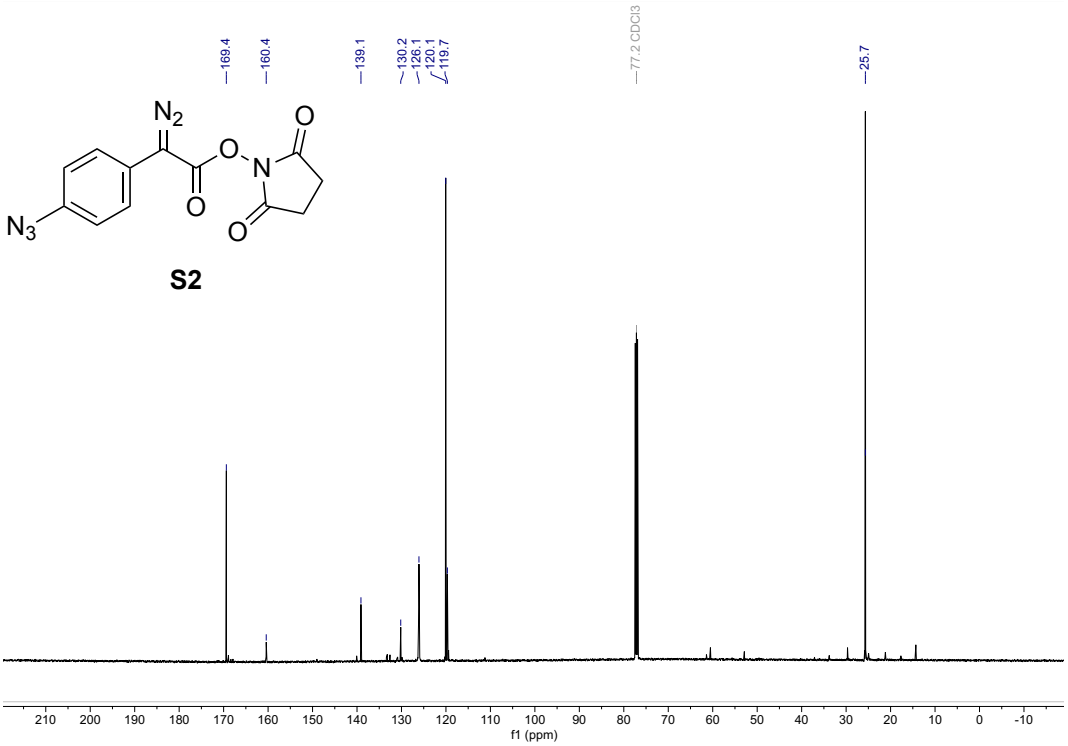

S2

^{1}H NMR (400 MHz) spectrum of diazo compound **1** in $CDCl_3$

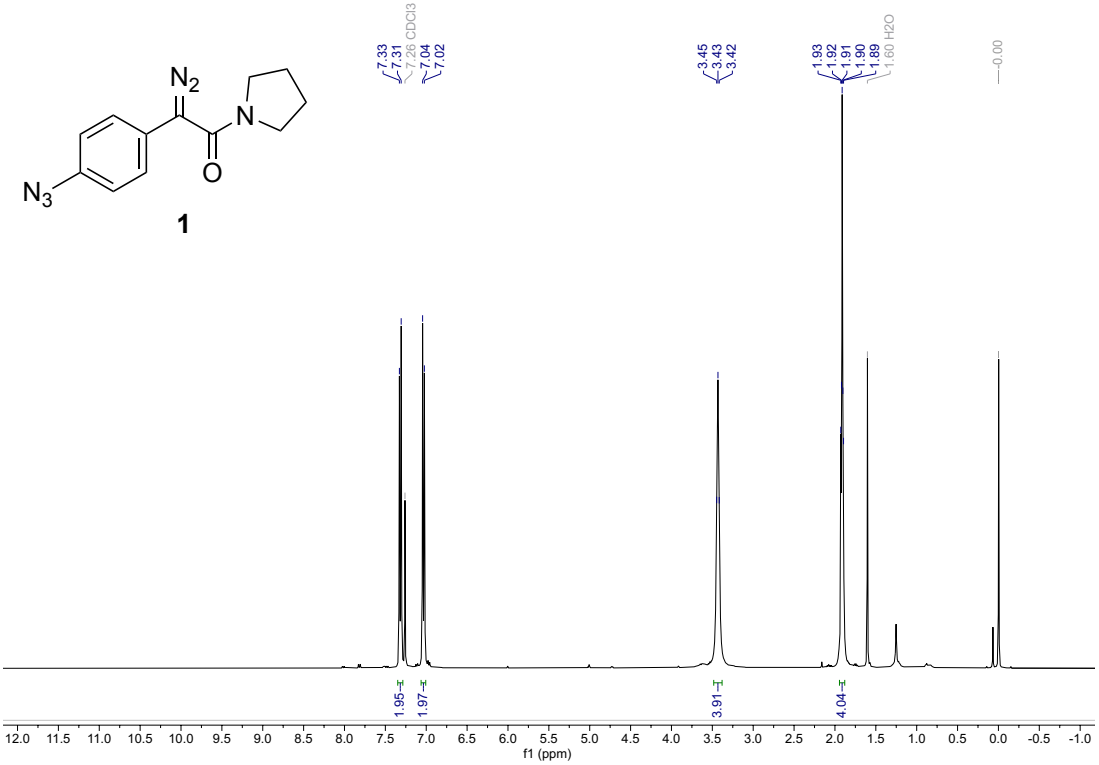

^{13}C NMR (101 MHz) spectrum of diazo compound **1** in $CDCl_3$

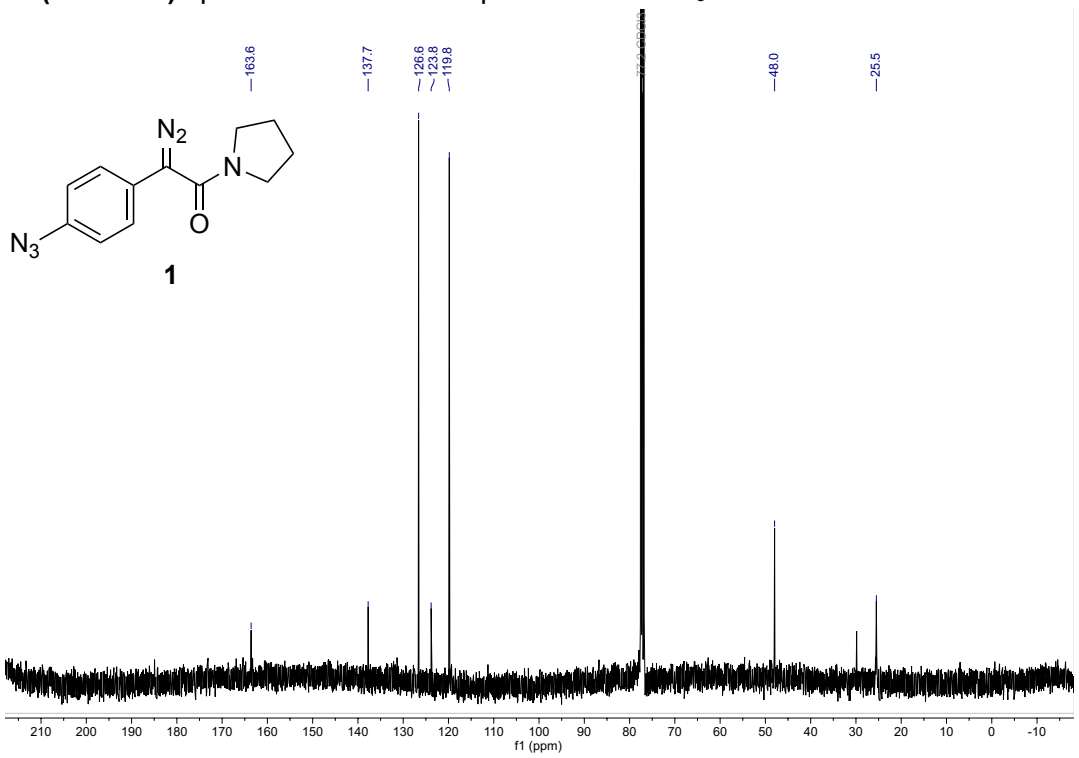

11. References

[1] W. D. Butt, D. Keilin, *Proc. R. Soc. B: Biol. Sci.* **1962**, *156*, 429–458.
[2] J. V. Jun, R. T. Raines, *Org. Lett.* **2021**, *23*, 3110–3114.
[3] A. Ouihia, L. Rene, J. Guilhem, C. Pascard, B. Badet, *J. Org. Chem.* **1993**, *58*, 1641–1642.
[4] S. P. Green, K. M. Wheelhouse, A. D. Payne, J. P. Hallett, P. W. Miller, J. A. Bull, *Org. Process Res. Dev.* **2020**, *24*, 67–84.
[5] For information on azide compounds, see: https://ehs.stanford.edu/reference/information-azide-compounds (accessed 21 October 2022).
[6] J. C. Cheetham, P. J. Artymiuk, D. C. Phillips, *J. Mol. Biol.* **1992**, *224*, 613–628.
[7] G. W. Bushnell, G. V. Louie, G. D. Brayer, *J. Mol. Biol.* **1990**, *214*, 585–595.
[8] M. Prabu-Jeyabalan, E. Nalivaika, C. A. Schiffer, *J. Mol. Biol.* **2000**, *301*, 1207–1220.
[9] A. K. Gupta, X. Yin, M. Mukherjee, A. A. Desai, A. Mohammadlou, K. Jurewicz, W. D. Wulff, *Angew. Chem. Int. Ed.* **2019**, *58*, 3361–3367.
[10] K. A. Mix, R. T. Raines, *Org. Lett.* **2015**, *17*, 2358–2361.
[11] G. R. Grimsley, J. M. Scholtz, C. N. Pace, *Protein Sci.* **2009**, *18*, 247–251.
[12] G. E. Briggs, J. B. S. Haldane, *Biochem. J.* **1925**, *19*, 338–339.
[13] A. N. Muttathukattil, P. C. Singh, G. Reddy, *J. Phys. Chem. B* **2019**, *123*, 3232–3241.
[14] N. D. Baker, R. J. Griffin, W. J. Irwin, J. A. Slack, *Int. J. Pharm.* **1989**, *52*, 231–238.
[15] B. Lukasak, K. Morihiro, A. Deiters, *Sci. Rep.* **2019**, *9*, 1470.
[16] M. Alapa, C. Cui, P. Shu, H. Li, V. Kholodovych, A. Beuve, *Free Radic. Biol. Med.* **2021**, *162*, 450–460.
[17] Y. Hamuro, S. J. Coales, K. S. Molnar, S. J. Tuske, J. A. Morrow, *Rapid Commun. Mass Spectrom.* **2008**, *22*, 1041–1046.
[18] S. König, *J. Mass Spectrom.* **2021**, *56*, e4616.
[19] B. Felding-Habermann, B. M. Mueller, C. A. Romerdahl, D. A. Cheresh, *J. Clin. Investig.* **1992**, *89*, 2018–2022.
[20] D. A. Cheresh, R. C. Spiro, *J. Biol. Chem.* **1987**, *262*, 17703–17711.
[21] L. Brocchieri, S. Karlin, *Nucleic Acids Res.* **2005**, *33*, 3390–3400.
[22] G. R. Moore, *FEBS Lett.* **1983**, *161*, 171–175.
[23] R. Timkovich, *Biochem. J.* **1980**, *185*, 47–57.
[24] R. T. Hartshorn, G. R. Moore, *Biochem. J.* **1989**, *258*, 595–598.
[25] W. D. Butt, D. Keilin, *Proc. R. Soc. B: Biol. Sci.* **1997**, *156*, 429–458.
[26] G. P. McStay, D. R. Green, *Cold Spring Harb. Protoc.* **2014**, 778–782.
[27] G. C. Brown, V. Borutaite, *Biochim. Biophys. Acta. – Biomembr.* **2008**, *1777*, 778–782.
[28] B. M. Hampton, B. Zhivotovsky, F. G. A. Slater, H. D. Burgess, S. Orrenius, *Biochem. J.* **1998**, *329*, 95–99.
[29] D. Alvarez-Paggi, L. Hannibal, M. A. Castro, S. Oviedo-Rouco, V. Demicheli, V. Tórtora, F. Tomasina, R. Radi, D. H. Murgida, *Chem. Rev.* **2017**, *117*, 13382–13460.
[30] I. W. Windsor, R. T. Raines, *Acta Crystallogr. D* **2018**, *74*, 690–694.
[31] J. M. Louis, L. Deshmukh, J. M. Sayer, A. Aniana, G. M. Clore, *Biochemistry* **2015**, *54*, 5414–5424.
[32] B. Mahalingam, J. M. Louis, J. Hung, R. W. Harrison, I. T. Weber, *Proteins: Struct. Funct. Genet.* **2001**, *43*, 455–464.
[33] I. W. Windsor, R. T. Raines, *Sci. Rep.* **2015**, *5*, 11286.

[34] J. O. Hui, A. G. Tomasselli, I. M. Reardon, J. M. Lull, D. P. Brunner, C.-S. C. Tomich, R. L. Heinrikson, *J. Protein Chem.* **1993**, *12*, 323–327.
[35] M. J. Todd, N. Semo, E. Freire, *J. Mol. Biol.* **1998**, *283*, 475–488.
[36] G. F. Short, M. Lodder, A. L. Laikhter, T. Arslan, S. M. Hecht, *J. Am. Chem. Soc.* **1999**, *121*, 478–479.
[37] T. D. McGee, Jr., J. Edwards, A. E. Roitberg, *J. Phys. Chem. B* **2014**, *118*, 12577–12585.
[38] F. Hofer, J. Kraml, U. Kahler, A. S. Kamenik, K. R. Liedl, *J. Chem. Inf. Model.* **2020**, *60*, 3030–3042.
[39] L. J. Hyland, T. A. Tomaszek, T. D. Meek, *Biochemistry* **1991**, *30*, 8454–8463.
[40] R. Smith, I. M. Brereton, R. Y. Chai, S. B. H. Kent, *Nat. Struct. Biol.* **1996**, *3*, 946–950.
[41] E. Ido, H. P. Han, F. J. Kezdy, J. Tang, *J. Biol. Chem.* **1991**, *266*, 24359–24366.
[42] D. W. Kneller, J. Agniswamy, R. W. Harrison, I. T. Weber, *FEBS J.* **2020**, *287*, 3235–3254.
[43] J. M. Sayer, F. Liu, R. Ishima, I. T. Weber, J. M. Louis, *J. Biol. Chem.* **2008**, *283*, 13459–13470.
[44] P. L. Darke, D. L. Hall, S. P. Jordan, J. A. Zugay, J. A. Shafer, L. C. Kuo, *Biochem.* **1994**, *33*, 98–105.